

CHAPTER 1

Carbon Nanotube/Nanofibre Polymer Composites

Milo S.P. Shaffer¹ and Jan K.W. Sandler²

¹*Department of Chemistry, Room 103d RCSI
Imperial College London, SW7 2AZ, UK
Tel: +44(0)20 7594 5825; Fax: +44(0)20 7594 5801
m.shaffer@imperial.ac.uk*

²*Polymer Engineering, University of Bayreuth
Universitätsstrasse 30, D-95447 Bayreuth, Germany
jan.sandler@uni-bayreuth.de*

1. Introduction

Although the terms *nanomaterial* and *nanocomposite* represent new and exciting fields in materials science, such materials have actually been used for centuries and have always existed in nature. However, it is only recently that the means to characterise and control structure at the nanoscale have stimulated rational investigation and exploitation. A nanocomposite is defined as a composite material where at least one of the dimensions of one of its constituents is on the nanometre size scale [1]. The term usually also implies the combination of two (or more) distinct materials, such as a ceramic and a polymer, rather than spontaneously phase-segregated structures. The challenge and interest in developing nanocomposites is to find ways to create macroscopic components that benefit from the unique physical and mechanical properties of very small objects within them.

Natural materials such as bone, tooth, and nacre are very good examples of the successful implementation of this concept, offering excellent mechanical properties compared to those of their constituent materials. Such composites actually exhibit beautifully organised levels of hierarchical structure from macroscopic to microscopic length scales,

and provide a powerful motivation for improving our processing control. Currently, we are striving to understand the behaviour of just the smallest building blocks in such materials which are the natural versions of nanocomposites. Significantly, two contrasting phases are often combined: a hard nanoscale reinforcement (such as hydroxyapatite or calcium carbonate) is embedded in a soft, usually protein-based, matrix. Although the composite character of these materials itself plays a crucial role, the question remains, why the nanometre scale is so important.

From a simple mechanical point of view, the situation in such biocomposites is quite familiar: the matrix transfers the load via shear to the nanoscale reinforcement [2]. A large length-to-diameter (aspect) ratio of the mineral reinforcement compensates for the low modulus of the soft protein matrix, leading to an optimised stiffness of the composite. The fracture toughness of such biocomposites, on the other hand, hinges on the ultimate tensile strength, σ_r , of the reinforcement. Crucially, the use of a nanomaterial allows access to the maximum theoretical strength of the material, since mechanical properties become increasingly insensitive to flaws at the nanoscale [2]. This observation is an extension of the classic approach to strong materials, namely to reduce the dimensions until critical flaws are excluded. At the nanoscale, highly crystalline reinforcements are used in which all but the smallest atomistic defects can be eliminated. It is clear that a high aspect ratio must be maintained in order to ensure suitable stress transfer. This general concept of exploiting the inherent properties of nanoscaled materials is not limited to the mechanical properties of a material, since a wide range of physical properties also depend on defect concentrations. In addition, the small size scale can generate inherently novel effects through, for example, quantum confinement, or through the dramatic increase in interfacial area.

The concept of creating both structural and functional multi-phase nanocomposites with improved performance is currently under development in a wide variety of metallic, ceramic, and polymeric matrices, although the emphasis to date has been on polymeric systems. Similarly, the filler particles can be organic or inorganic with a wide range of material compositions and structures. The resulting composites generally exhibit a number of enhanced properties, so that the material

cannot easily be classified as a structural or functional composite. The term *reinforcement*, as opposed to plain *filler*, is equally frequently used for the nanoscale component, without a clear distinction.

Carbon nanotubes (CNTs) have attracted particular interest because they are predicted, and indeed observed, to have remarkable mechanical and other physical properties. The combination of these properties with very low densities suggests that CNTs are ideal candidates for high-performance polymer composites; in a sense they may be the next generation of carbon fibres. Although tens or hundreds of kilograms of carbon nanotubes are currently produced per day, the development of high-strength and high-stiffness polymer composites based on these carbon nanostructures has been hampered so far by the lack of availability of high quality (high crystallinity) nanotubes in large quantities. In addition, a number of fundamental challenges arise from the small size of these fillers. Although significant advances have been made in recent years to overcome difficulties with the manufacture of polymer nanocomposites, processing remains a key challenge in fully utilising the properties of the nanoscale reinforcement. A primary difficulty is achieving a good dispersion of the nanoscale filler in a composite, independent of filler shape and aspect ratio. Without proper dispersion, filler aggregates tend to act as defect sites which limit the mechanical performance; such agglomerates also adversely influence physical composite properties such as optical transmissivity.

When dispersing small particles in a low viscosity medium, diffusion processes and particle-particle and particle-matrix interactions play an increasingly important role as the diameter drops below 1 μm . It is not only the absolute size but rather the specific surface area of the filler, and the resulting interfacial volumes, which significantly influence the dispersion process. These regions can have distinctly different properties from the bulk polymer and can represent a substantial volume fraction of the matrix for nanoparticles with surface areas of the order of hundreds of m^2/g . The actual interphase volume depends on the dispersion and distribution of the filler particles, as well as their surface area.

In traditional fibre composites, the interfacial region is defined as the volume in which the properties deviate from those of the bulk matrix or

filler [3]. However, it is simpler, in the case of small particles, to consider a straightforward calculation [4] of the interparticle distance s :

$$s = d^* \left[\left(\frac{\pi}{6\phi_V} \right)^{1/3} - 1 \right], \quad (1)$$

where d is the diameter and ϕ_V is the volume fraction of uniformly-sized, spherical particles on a lattice. As an example, a 15 vol% loading of 10 nm diameter particles leads to an interparticle distance of only 5 nm. This figure, which is similar to the radius of gyration of a typical polymer molecule, shows that essentially the entire polymer matrix in a nanocomposite can behave as if it were part of an ‘interphase’. In other words, the properties of the whole matrix may differ from the pure bulk polymer in terms of the degree of cure, chain mobility, chain conformation, and degree of chain ordering or crystallinity. These effects may influence both processing and final properties of the polymeric phase. One simple but important consequence is that it becomes increasingly difficult to ‘wet’ adequately all of the nanofiller surface with polymer; thus, the volume fraction of nanomaterial that can be uniformly dispersed using conventional processing techniques is decreased. In addition, the strong influence of interfacial interactions during processing can alter the matrix microstructure which, particularly in the case of semicrystalline polymers, can significantly affect the mechanical behaviour of the nanocomposite independently of direct load-bearing by the filler [5]. Therefore, the matrix microstructure must be critically assessed when evaluating the performance of carbon nanotube-polymer composites. Although the high aspect ratio of carbon nanotubes generally appears to be a clear benefit for the exploitation of their mechanical as well as physical properties such as electrical conductivity, it is as yet not established which of the many different types of nanotubes will yield the ultimate performance in a polymer composite. Nanotubes have shown a remarkable range of structural features, and the resulting structure-property-relationships are only slowly emerging.

2. Carbon Nanotubes and Nanofibres

Carbon nanotubes are often seen as the intersection of traditional carbon fibres with the fullerene family [6]. It was only realised relatively recently that solids of pure elemental carbon with sp^2 -hybridisation can form a wide variety of well-defined crystalline structures. The first recognition of the fullerenes as closed structures [7] in 1985, and their subsequent synthesis in a carbon arc [8], stimulated enormous new interest in carbon materials. In 1991, Iijima observed a graphitic tubular structure in an arc discharge apparatus that was used to produce C_{60} and other fullerenes. His realisation [9] of the structural richness of these particles, which came to be known as nanotubes, generated enormous interest; indeed, there are now in excess of 10,000 papers discussing the science of CNTs, including a large fraction on polymer composites. Although Iijima is often credited with the discovery of CNTs, there are earlier reports in the literature, notably by Endo in 1976, of the synthesis of tubular carbon structures using hydrocarbon decomposition [10]. There are even reports in the catalysis literature of the 1950s of attempts to remove troublesome fibrous carbon deposits. The electric arc method was actually used as early as 1960 by Roger Bacon [11] to produce graphite whiskers, and one can also speculate that nanotubes were likely present in his experiments as a by-product, although unobserved. The explosion of interest in 1991 was driven by the renewed interest in carbon following the discovery of fullerenes, and the structural perfection of Iijima's nanotubes which implied a whole range of exciting properties.

CNTs have typical diameters in the range of ~ 1 –50 nm and lengths of many microns (even centimetres in special cases). They can consist of one or more concentric graphitic cylinders. In contrast, commercial (PAN and pitch) carbon fibres are typically in the 7–20 μm diameter range, while vapour-grown carbon fibres (VGCFs) have intermediate diameters ranging from a few hundred nanometres up to around a millimetre. The variation in diameter of fibrous graphitic materials is summarised in Figure 1. Crucially, conventional carbon fibres do not have the same potential for structural perfection that can be observed in CNTs. Indeed, there is a general question as to whether the smallest

CNTs should be regarded as very small fibres or heavy molecules, since the diameters of the smallest nanotubes are similar to those of common polymer molecules. This ambiguity is characteristic of nanomaterials, and it is not yet clear to what extent conventional fibre composite understanding can be extended to CNT composites.

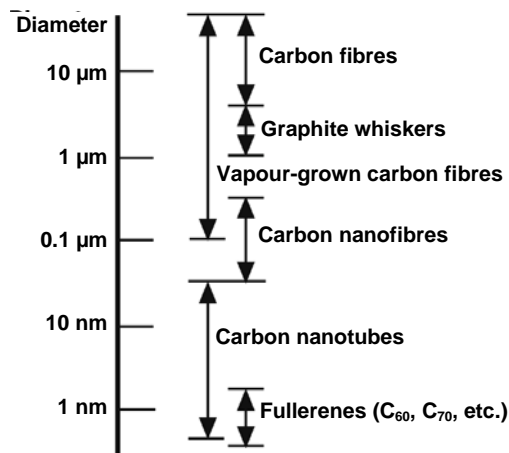


Fig. 1. Comparison of diameters of various fibrous carbon-based materials.

The nanotube structure can be defined more exactly by considering a single-wall carbon nanotube (SWCNT) as a conformal mapping of the two-dimensional hexagonal lattice of a single graphene sheet onto the surface of a cylinder. The graphite sheet may be 'rolled' in different orientations along any two-dimensional lattice vector (m,n) which then maps onto the circumference of the resulting cylinder; the orientation of the graphite lattice relative to the axis defines the *chirality* or *helicity* of the nanotube [12]. As-grown, each nanotube is closed at both ends by a hemispherical cap formed by the replacement of hexagons with pentagons in the graphite sheet which induces curvature. SWCNTs are usually obtained in the form of so-called ropes or bundles, containing between 20 and 100 individual tubes packed in a hexagonal array [13–16]. Rope formation is energetically favourable due to the Van der Waals attractions between isolated nanotubes [17]. Multi-wall carbon nanotubes (MWCNTs) provide an alternative route to stabilisation. They consist of

two or more coaxial cylinders, each rolled out of single sheets, separated by approximately the interlayer spacing in graphite. The outer diameter of such MWCNTs can vary between 2 and a somewhat arbitrary upper limit of about 50 nm; the inner hollow core is often (though not necessarily) quite large with a diameter commonly about half of that of the whole tube. Carbon nanofibres (CNFs) are mainly differentiated from nanotubes by the orientation of the graphene planes: whereas the graphitic layers are parallel to the axis in nanotubes, nanofibres can show a wide range of orientations of the graphitic layers with respect to the fibre axis. They can be visualised as stacked graphitic discs or (truncated) cones, and are intrinsically less perfect as they have graphitic edge terminations on their surface. Nevertheless, these nanostructures can be in the form of hollow tubes with an outer diameter as small as ~5 nm, although 50–100 nm is more typical. The stacked cone geometry is often called a ‘herringbone fibre’ due to the appearance of the longitudinal cross-section. Slightly larger (100–200 nm) fibres are also often called CNFs, even if the graphitic orientation is approximately parallel to the axis. Representative transmission electron micrographs of commercially available nanofibres with a mean outer diameter of around 150 nm are shown in Figure 2. The schematic diagram highlights the orientation of the graphitic planes in the inner and outer regions of the nanofibre wall, and is intended to illustrate the structural complexity that can arise in these materials.

A variety of synthesis methods now exist to produce carbon nanotubes and nanofibres. However, these carbon nanostructures differ greatly with regard to their diameter, aspect ratio, crystallinity, crystalline orientation, purity, entanglement, surface chemistry, and straightness. These structural variations dramatically affect intrinsic properties, processing, and behaviour in composite systems. However, it is not yet clear which type of nanotube material is most suitable for composite applications, nor is there much theoretical basis for rational design. Ultimately, the selection will depend on the matrix material, processing technology, and the property enhancement required. Thus, in order to interpret the data obtained for nanotube composites, and to develop the required understanding, it is essential to appreciate the range of nanotube materials available.

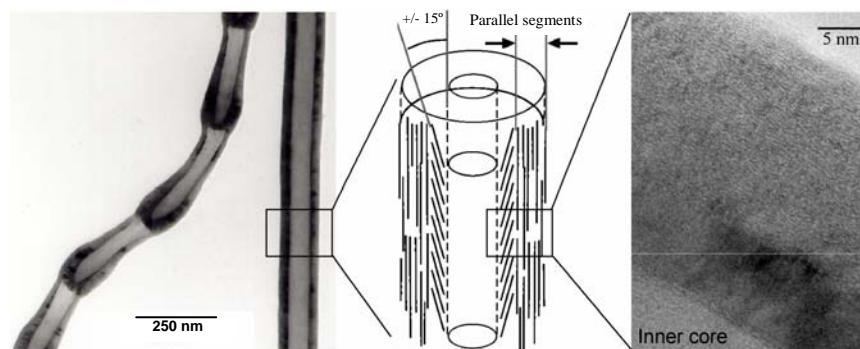


Fig. 2. Representative transmission electron micrographs of commercial carbon nanofibres, highlighting structural variations both in overall morphology and in the orientation of the graphitic planes. The leftmost image shows a ‘bamboo’ and a ‘cylindrical’ CNF, whilst the rightmost image shows a high magnification image of one wall of the cylindrical fibre which reveals the graphitic arrangement sketched in the central panel.

2.1. Production methods

Both MWCNTs and SWCNTs can be produced by a variety of different processes which can broadly be divided into two categories: high-temperature evaporation using arc-discharge [13,14,18–20] or laser ablation [15,21], and various chemical vapour deposition (CVD) or catalytic growth processes [16,22–24]. In the high-temperature methods MWCNTs can be produced from the evaporation of pure carbon, but the synthesis of SWCNTs requires the presence of a metallic catalyst. The CVD approach requires a catalyst for both types of CNTs but also allows the production of CNFs. Many variants exist, but the basic methods can be described as follows.

The electric arc method is based on the generation of a DC arc plasma between two carbon electrodes in an inert (usually helium) atmosphere. While the anode is consumed, a soft, dark black, fibrous deposit forms on the cathode which consists of about 50 vol% straight MWCNTs, often arranged in a fractal structure. Addition of a suitable catalyst such as Ni-Co, Co-Y or Ni-Y leads to the formation of interconnected web-like SWCNT bundles on the walls of the reaction chamber [13,14,25,26]. Macroscopically long ropes of well-aligned SWCNTs can be synthesised

by the arc-discharge method using hydrogen [27]. Laser ablation is a similar process, using a different technique to generate the carbon vapour; although the method can generate MWCNTs, it is usually used for the production of SWCNTs at yields higher than 70%. A graphite target, containing a 1–2% metal catalyst, is held in a furnace at 1200°C in an inert atmosphere and is evaporated using a high power laser [15,28]. The resulting products are swept from the high-temperature zone by the flowing inert gas and are deposited on a conical water-cooled copper collector.

The products of both high-temperature routes tend to be highly crystalline, with low defect concentrations, but are relatively impure, containing other, unwanted carbonaceous impurities. These methods usually work on the gram scale and are, therefore, relatively expensive. For the use of nanotubes in composites, large quantities of nanotubes are required at low cost, ideally without the requirement for complicated purification. At present, only CVD-grown nanotubes satisfy these requirements and, as such, tend to be the materials of choice for composite work, both in academia and in industry. The main contaminants in CVD materials are residual catalyst particles which are mostly incorporated into the nanotubes. On the other hand, these gas-phase processes operate at lower temperatures and lead to structurally more imperfect nanotubes, as shown by the deviation from the ideal cylindrical structure in Figure 3.

Carbon filaments can form when small metal particles, almost always containing iron, nickel, or cobalt, are exposed to CO or hydrocarbon gases at temperatures between 500 and 1200°C. The carbonaceous feedstock decomposes on the catalyst, generating carbon which diffuses through or around the catalyst to produce a fibre with a diameter similar to the metal particle [29]. Originally, the method was developed for growing VGCFs with diameters up to several hundred micrometres through simultaneous pyrolytic overgrowth on the primary fibre. Later, various orientations of the graphitic planes with respect to the fibre axis were observed depending on the crystallographic orientation of the catalyst particle [30]. The arrangement of the graphitic planes can vary from perpendicular to the fibre axis to parallel, thus generating a range of

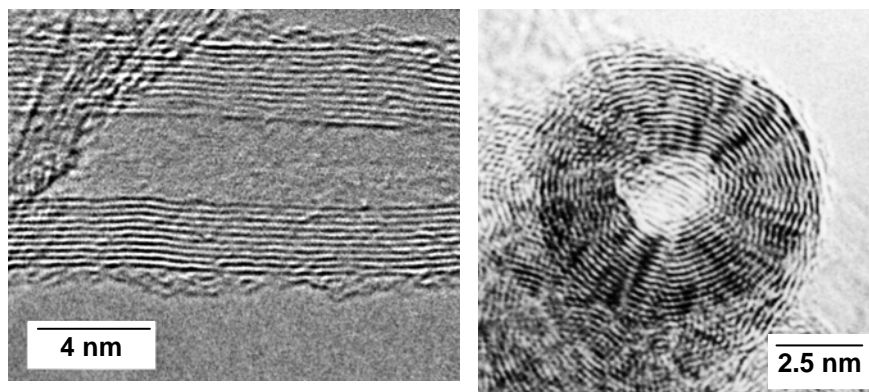


Fig. 3. Transmission electron micrographs of commercial MWCNTs grown by CVD methods, with the beam perpendicular (left) and parallel (right) to the axis.

CNF structures [31]. Twisted, helical, and branched nanofibres have also been reported [32].

Under the right conditions, entangled mats of catalytically-grown CNTs can be produced [22]. Generally, the experiment is carried out in a flow furnace at atmospheric pressure [33,34]. In perhaps the simplest embodiment, the catalyst is placed in a ceramic boat which is then put into a quartz tube. A reaction mixture consisting of, for example, acetylene and argon is passed over the catalyst bed for several hours at temperatures ranging from 500 to 1100°C [34]. In fact, there are many options for introducing the catalyst ranging from injection of organometallic vapours and metallic colloids, to pre-deposition of metal films or particles on ceramic supports. Injecting the catalyst into the gas stream allows for the continuous production of nanotubes. A number of commercial routes to the production of vapour-grown CNFs and CNTs are based on a ‘floating catalyst’ carried in the gas stream inside a continuous flow reactor [35].

The CVD products discussed above tend to be highly entangled; however, aligned nanotube arrays, as shown in Figure 4a, can be obtained under conditions that lead to rapid and dense nucleation on flat substrates [36–39]. With sufficient growth time, lengths in the millimetre

range have been observed [40]. Such aligned MWCNT films can be easily removed from the substrate and might be considered as the ideal nanotube material for composite applications, as the low degree of nanotube entanglement should allow straightforward dispersion in a polymer matrix. The synthesis of well-aligned and comparatively straight MWCNTs on substrates can be further enhanced by the application of a plasma during growth [41,42]. This approach has recently been shown to allow the production of aligned nanotube films at temperatures as low as 120°C [43], opening the door for direct nanotube growth on polymer substrates. The use of plasma accelerates growth, and increases alignment, but tends to reduce crystallinity.

Although a number of commercial CVD routes to SWCNTs exist, the so-called 'HiPco' process has received particular attention. The gas-phase growth of SWCNTs using high-pressure carbon monoxide as the carbon source was developed by Nikolaev *et al.* [44] but is now commercially exploited by Carbon Nanotechnologies Inc., USA. The product is shown in Figure 4b and is widely used for research purposes, although it is, at present, still too expensive for large-scale commercial composite applications.

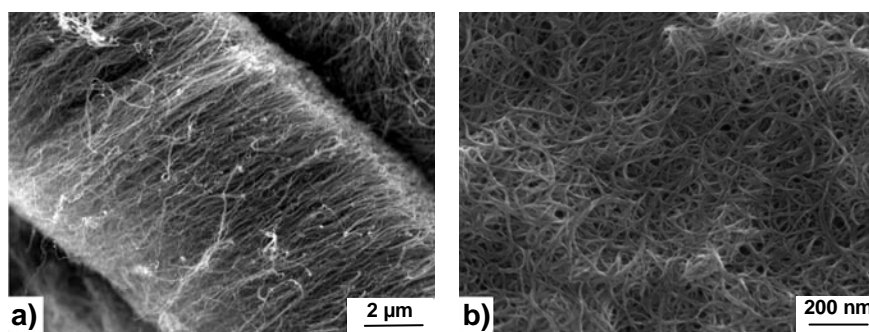


Fig. 4. Scanning electron micrographs of (a) aligned multi-wall carbon nanotubes and (b) HiPco single-wall carbon nanotubes produced by CVD methods.

In summary, the quality and yield of carbon nanotubes depend on the synthesis technique and the specific growth conditions used. Catalytic processes generally involve lower growth temperatures which lead to

both variations in the orientation of the graphitic planes with respect to the tube axis and to an increased concentration of structural defects. It is not surprising that most studies aimed at investigating the fundamental mechanical and physical properties of individual nanotubes have been performed on high-temperature materials with few structural defects. Relatively little effort has been applied to CNFs, although given their structural appearance, their properties should, at best, resemble those of very defective catalytic nanotubes.

2.2. Mechanical properties of carbon nanotubes

Although challenging, a number of experimental studies have focussed on the direct determination of the mechanical properties of individual carbon nanotubes. Experimental measurements of nanotube deformations have mostly been analysed by assuming nanotubes to be elastic beams. The resulting elastic constants belong to the framework of continuum elasticity, and any estimate of these material parameters for nanotubes therefore implies the continuum assumption. There is also a general question as to what should be taken as the cross-section of a nanotube. For MWCNTs, values have usually been calculated based on a thick-walled cylinder, ignoring the cross-section of the hollow core, although it might be argued that the area of the core should be included since it is an intrinsic feature of the structure. The question is even more difficult with SWCNTs which are only a single layer of atoms thick. Usually, the thickness, t , is taken to be the interlayer spacing of graphite, although difficulties with bending stiffness remain [45].

The original determinations of CNT stiffness were based on observing the amplitude of thermal vibrations in a TEM; average stiffness values of 1.8 TPa [46] and 1.25 TPa [47] were obtained for MWCNTs and SWCNTs, respectively. For MWCNTs, the estimated nanotube stiffness appeared to depend on the diameter [48], an effect that was explained by the occurrence of wave-like distortions for multi-wall carbon nanotubes with diameters of greater than 12 nm, as predicted by a combination of finite element analysis and non-linear vibration analysis

[49]. Falvo *et al.* [50] showed that MWCNTs could be repeatedly bent to large angles ($> 120^\circ$) with an AFM tip without undergoing catastrophic failure; this observation was supported by high-resolution TEM studies that indicated reversible buckling as a mechanism for stress relief [51–53]. Lourie *et al.* captured the buckling of SWCNTs in compression and bending by embedding the nanotubes in a polymer film [54].

Static models of beam bending have also been used to quantify mechanical properties of nanotubes. AFM measurements led to an average bending stiffness of arc-grown MWCNTs of about 1 TPa [55,56]; however, catalytic nanofibres with a higher defect concentration were found to have a substantially lower stiffness of only 10 to 50 GPa [56]. Whereas point defects do not affect the nanotube stiffness greatly, deviations from a perfectly parallel alignment of the graphitic layers to the axis have a significant detrimental effect on properties, due to the high anisotropy of graphite.

More recently, a mechanical loading stage operating inside an SEM was used to perform the first *in-situ* tensile tests on individual MWCNTs and ropes of SWCNTs. Individual arc-grown MWCNTs were found to fracture by a so-called *sword-in-sheath* mechanism in the outermost shell. Strength values for the outer shell ranged from 11 to 63 GPa at fracture strains of up to 12% and modulus values ranged from 270 to 950 GPa [57]. By assuming that the load is carried only by the SWCNTs on the perimeter of the rope, fracture strengths ranging from 13 to 52 GPa and moduli between 320 and 1470 GPa were obtained [58]. It is interesting to note that the maximum fracture strain was found to be 5.3% which is close to the theoretical value of $\sim 5\%$ for defect nucleation in individual SWCNTs [59].

The experimental results for highly crystalline nanotubes (produced by high-temperature methods) show that such nanotubes can indeed have a Young's modulus approaching the theoretical value of 1.06 TPa [52], the in-plane modulus of graphite, in agreement with theoretical studies [60,61]. (Young's modulus values of around 5.5 TPa [46] relate to an assumed effective SWCNT wall thickness of 0.066 nm). It should be borne in mind that a single value of Young's modulus should not be uniquely used to describe both the tension/compression *and* bending

behaviour of carbon nanotubes. Tension and compression are mostly governed by the in-plane σ -bonds, while pure bending is affected by the out-of-plane π -bonds. However, within a given mode, continuum elasticity does seem to be applicable to the elastic properties of such nanostructures, up to the point at which local instabilities occur, as long as the geometry of the nanotubes is properly taken into account.

A number of theoretical studies have addressed the structural stability of nanotubes in tension, compression, bending, and torsion. Under axial loads, abrupt changes in nanotube morphology were observed which depended on the nanotube length [62,63]. Nanotube buckling due to bending has also been demonstrated [62,64] and is characterised by a collapse of the cross-section in the middle of the tube, in agreement with experimental observations [51–53].

The strength of nanotubes depends on the distribution of defects, as well as interlayer interactions in MWCNTs and bundles of SWCNTs. The defect density is potentially low in these nanostructures and defect sites may be distributed over large distances due to the small diameter and high aspect ratio. However, defect density will depend on the growth process, and the strength should only approach the theoretical limit for nanotubes grown at high-temperatures. There are relatively few experimental results but those mentioned above are in good agreement with theoretical predictions [65] and indeed indicate that the strength of nanotubes can be one order of magnitude higher than that of current high-strength carbon fibres. Further evidence for the high strength of high temperature nanotubes has been found in other tensile tests [66], although the strength decreased significantly for 2 mm long bundles of MWCNTs grown in a CVD process [67]. In this case, the average strength of about 1.7 GPa might be related to the higher defect concentration as a result of the lower growth temperature, but could also be attributed to gauge length effects, with individual nanotubes being shorter than the overall length of the bundle. Initial fragmentation tests of nanotubes embedded in thin film polymer composite films also led to an estimated high tensile strength of nanotubes [68,69], although an accurate determination of the fragment length of an embedded nanotube in a TEM sample is challenging.

Although the high nanotube strength is derived from the strong in-plane graphitic bonds, the weak interlayer interactions may cause problems. MWCNTs appear to fall victim to their own in-plane structural perfection which minimises load transfer to the inner shells when the outermost shell is strained in tension. Whether end effects, high aspect ratios, or modest defect concentrations can alleviate this problem remains to be seen. Similarly, the inner SWCNTs in a bundle may not contribute to the overall mechanical performance. For these reasons, some have suggested that individually dispersed SWCNTs should be the ideal reinforcement. Experimentally, these ideas are supported by the failure mechanisms observed in individual CNT tensile tests and by some composite data. For example, macroscopic epoxy samples containing 5 wt% of dispersed MWCNTs subjected to tensile and compressive loads showed a more pronounced modulus enhancement in compression; the result is consistent with the idea that only the outer nanotube layers are stressed in tension, whereas all layers contribute under compression [70].

2.3. Transport properties of carbon nanotubes

The electronic properties of nanotubes are another area of great scientific interest, yet they are also challenging to measure directly on individual CNTs. Structural defects as well as bends or twists are again thought to have a strong effect on the transport properties [71]. Initial theoretical studies of the electronic properties of SWCNTs, based on band-folding, indicated that nanotube shells can be either metallic or semiconducting depending critically on helicity [72–74], with a small or moderate band gap (for semiconducting tubes) inversely proportional to the tube radius [75,76]. On average, approximately 1/3 of SWCNTs are metallic and 2/3 semiconductors [72]; this ratio tends to be observed in real samples because current synthesis methods offer little, if any, control over helicity. Since MWCNTs have larger diameters, confinement effects disappear, and the transport properties approach those of turbostratic graphite [77]. Interlayer interactions which might be important in small diameter MWCNTs appear to be weak; theoretical studies of double-wall nanotubes indicate that the overall behaviour is determined by the electronic properties of the external shell [78,79].

Results of experimental transport measurements of nanotubes, therefore, vary strongly between individual SWCNTs, SWCNT bundles, individual MWCNTs, or MWCNT bundles or mats. Connections to individual CNTs are usually made either by random deposition of CNTs on pre-patterned electrodes [80,81], or subsequent deposition of contacts using focussed ion beam techniques [82]. The first experimental transport measurement of individual SWCNTs was carried out by Tans *et al.* [83] and showed that there are indeed metallic and semiconducting SWCNTs, verifying the theoretical predictions. The room temperature conductivity was about 10^5 to 10^6 S/m for the metallic nanotubes and about 10 S/m for semiconducting tubes. Scanning tunnelling spectroscopy verified experimentally that the electronic properties sensitively depend on nanotube diameter and helicity [84,85], and that there is no preferred helicity in laser-grown SWCNT material [84]. The presence of a large fraction of semiconducting tubes should therefore be considered when interpreting transport measurements on bundles of SWCNTs, as verified experimentally by a temperature-dependent resistivity of bundles [86]. The conductivity of SWCNT bundles was found to vary between 1×10^4 [87] and 3×10^6 S/m [88,89] at room temperature, depending on sample type and entanglement state. These values approach that for the in-plane conductivity of graphite (2.5×10^6 S/m [90]). Conductivities of individual MWCNTs have been reported to range between 20 and 2×10^7 S/m [82], depending on the helicities of the outermost shells [91] or the presence of defects [92]. The electronic properties of larger diameter MWCNTs approach those of graphite.

Remarkable similarities between the conductivity behaviour of nanotube networks and conducting polymers have been pointed out by Kaiser *et al.* [93]. In analogy to conducting polymers, a good description of the experimentally observed conductivity behaviour is given by a simple model of metallic conduction with hopping or tunnelling through small electrical barriers, e.g. tangled regions, inter-rope or intertube contacts, or tube defects.

Lastly, the axial thermal conductivity of individual, perfect CNTs is expected to be very high [94], greater than that of diamond, with experimental values for MWCNTs reaching 3300 W/m/K [95].

3. Carbon Nanotube/Nanofibre-reinforced Polymer Composites

There are at least three general experimental methods to produce polymer nanocomposites: mixing in the liquid state, solution-mediated processes and *in-situ* polymerisation techniques. The direct melt-blending approach is much more commercially attractive than the latter two methods, as both solvent processing and *in-situ* polymerisation are less versatile and more environmentally contentious.

The literature on processing and evaluating macroscopic nanotube/nanofibre-polymer composites is still in its infancy but developing rapidly. This situation is not surprising, given that initial attempts to produce such nanocomposites were hindered by the small quantities of nanotubes available; although, more recently, the focus on CVD synthesis techniques has enabled the manufacture of large-scale polymer nanocomposites. As yet, no standard approach has been established to assess the resulting nanocomposite properties or to correlate them with the intrinsic nanotube characteristics. For example, a large number of studies have focussed on the effect of nanotubes and nanofibres on the composite stiffness, failing to report other, more relevant, properties such as strength and strain to failure. Such mechanical properties are more dependent on filler dispersion, alignment, and interface than the stiffness, and are more difficult both to improve and to analyse. Nevertheless, a number of interesting studies have been reported that illuminate the potential of nanotube and nanofibre composites.

3.1. Thermosetting carbon nanotube/nanofibre composites

Thermosetting epoxies have found a widespread use in applications ranging from household glues to high-performance composites. Increases in toughness, glass transition temperature (T_g), and mechanical properties above T_g would be of particular technological benefit. Initial experimental studies of nanotube-based thermosetting nanocomposites focussed on the production of thin epoxy films which required only small amounts of filler and provided information about dispersion and

interfacial properties. When using thermosetting matrices, as-received nanotubes are often directly mixed with the liquid matrix (especially epoxy) precursors. Mechanical mixing can be aided by ultrasonication and vacuum-assisted processing is often applied to ensure defect-free composite samples for mechanical testing. Chemically-treated nanotubes are often first dispersed in surfactants or solvents to which the epoxy is added.

A first example of this approach was published by Ajayan *et al.* who dispersed arc-grown MWCNTs by mechanical mixing in an epoxy resin [96]. The composites were microtomed for investigation by TEM, resulting in individual MWCNTs aligned parallel to the cutting direction. This alignment, and the lack of nanotube fracture, was interpreted as an indication that the nanotubes are strong and that the nanotube-matrix interface is weak. However, samples prepared with harder epoxy resins did allow cutting of nanotubes for direct cross-sectional examination [97]. Similar epoxy samples have been used to determine intrinsic mechanical nanotube characteristics [54,68,98–100]; interfacial bonding was generally assumed to be good because the epoxy was observed to wet both MWCNTs and bundles of SWCNTs.

Only relatively low concentrations (< ~5 wt%) of nanotubes can easily be incorporated in thermosetting composites, due to rapidly increasing viscosity and subsequent processing difficulties, at higher loadings. Even well-dispersed, shortened nanotubes can form a stiff gel, simply in solvent, due to their high aspect ratio and resulting network-forming ability [101]; the large interaction volume may also increase the background viscosity of the solvent/matrix. A further problem is aggregation of the nanofiller, which is a major issue in all nanocomposites, even at modest loading fractions. The introduction of pure nanotubes into thermosetting resins tends to yield only moderate increases in stiffness, whilst the strength and strain to failure of the matrix are usually degraded. This poor performance is often attributed to poor dispersion and various processing remedies have been explored. One tactic is to use continual mechanical stirring or ultrasonication to prevent reagglomeration of nanotubes [102]. This approach has been shown to reduce the average MWCNT cluster size in epoxy composites and hence to improve the composite tensile stiffness, although the strain

to failure still tends to be reduced [103]. An alternative to mechanical agitation is to introduce a surfactant [104]. Composites containing as little as 1 wt% of surfactant-dispersed MWCNTs show an improved thermomechanical behaviour as compared to the pure nanotube material, although the surfactant itself decreases the storage modulus of the epoxy significantly. The combination of MWCNTs and surfactant can increase the composite T_g , providing evidence for an improved interaction between filler and matrix.

A third strategy for improved dispersion is to use chemical routes to directly functionalise the CNTs [105]. The end caps of both single and multi-wall nanotubes can be opened under oxidising conditions, leading to carboxyl, carbonyl, and hydroxyl groups both at the opened ends and at defects on the side walls. Such oxidised nanotubes show a better solubility and can form electrostatically stabilised colloidal dispersions in water as well as alcohols [101,106], leading to improved dispersions in epoxy systems [107]. An example of well-dispersed, oxidised multi-wall nanotubes in an epoxy is shown in Figure 5. One drawback of such acid treatments is that they degrade the length of individual nanotubes [107], although an associated reduction in SWCNT bundle diameter may be an advantage [108,109]. Further improvements in solubility can be achieved by fluorination [110], again leading to improvements in both the stiffness and strength, on the addition of 1 wt% of oxidised and fluorinated SWCNTs [105]. In addition to improving dispersion, chemical functionalisation can encourage direct covalent coupling between the CNTs and the matrix; one example is the use of amino-functionalised MWCNTs in epoxy systems to yield improved properties [111]. The improved mechanical performance in these functionalised systems may reflect both the enhanced dispersion and an increased interaction of the nanotube surface groups with the polymer.

Using larger CNFs allows the processing of thermosetting composites with higher loadings, up to about 20 wt%, with relatively little void content [112,113]; the increase most likely reflects the smaller surface area of nanofibres compared to nanotubes, as well as their greater tendency to break during shear processing. At these filler fractions, randomly oriented CNFs in epoxy have been found to be as effective

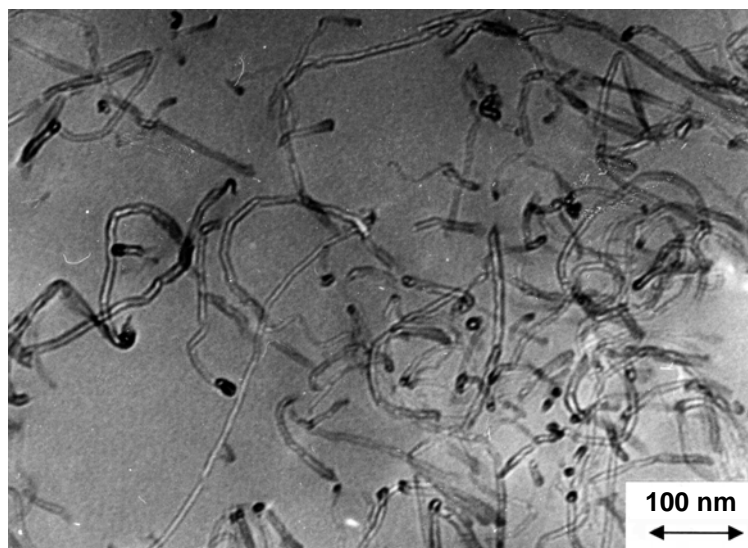


Fig. 5. Transmission electron micrograph of well-dispersed catalytically-grown multi-wall carbon nanotubes in an epoxy matrix as a result of a chemical oxidation treatment.

reinforcement as aligned short macroscopic VGCFs; a simple rule-of-mixture approach classified the CNFs as comparable to low modulus, medium-strength carbon fibres [112]. Interestingly, the CNFs were not as effective in a phenolic resin, possibly as a result of a better interfacial bonding in the epoxy composites [113].

The effect of nanotubes on either the curing reaction or the thermal degradation of thermosets has not yet been fully established. A change in curing is particularly relevant as the cross-link density has a pronounced influence on the mechanical performance, and nanotubes, particularly functionalised ones, both affect stoichiometry and act as massively parallel cross-linking sites. Acceleration of the epoxy cure reaction has been observed for untreated SWCNT bundles [114], the effect being most pronounced for low curing temperatures. This increase in reaction rate arises partly from the high thermal conductivity of the nanotubes but also depends on the specific surface area and surface chemistry, as shown by a comparative study of CNFs and carbon black [115]. The higher the degree of graphitisation of the filler surface, the less pronounced the effect on the curing rate. In addition, the presence of

SWCNTs degraded the thermal stability of the composite slightly [114]. Such effects still need to be addressed for chemically modified CNTs.

Both nanofibres and nanotubes have been used as electrically conductive fillers in epoxy composites [103,116–120]. Such composites display a characteristic percolation behaviour (see section 3.3.3 for a more detailed discussion in the context of thermoplastic nanocomposites). Both the percolation threshold and the maximum composite conductivity appear to depend on the type of nanoscale carbon filler and the degree of dispersion. In general, CNT-based composites have higher conductivities and lower percolation thresholds than either carbon black or CNF-based systems. Indeed, a CNT-filled epoxy currently shows the lowest percolation threshold observed in any system, at around 0.0025 wt% [121]. Figure 6 compares the best results achieved using MWCNTs from an aligned CVD-process with those obtained using entangled nanotubes and carbon black, in an aerospace grade epoxy

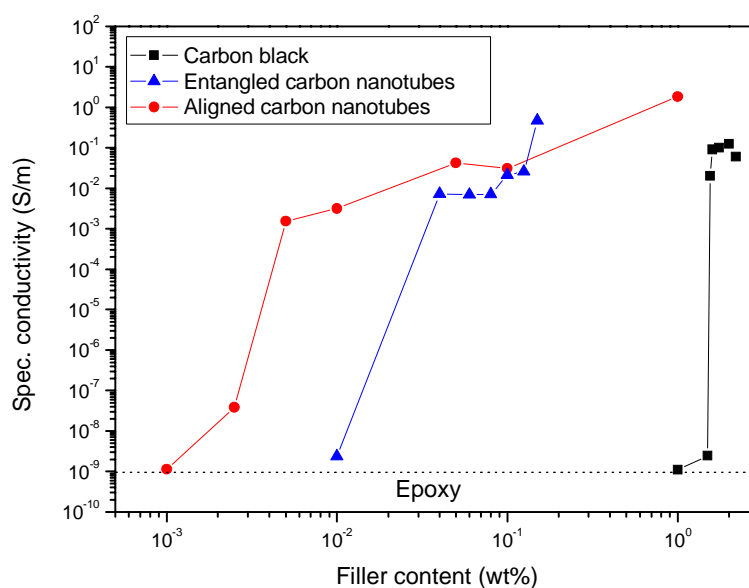


Fig. 6. Epoxy composite conductivity as a function of filler weight fraction for aligned CVD-grown multi-wall carbon nanotubes, compared to results obtained with commercially-available entangled nanotubes and carbon black particles.

system. It is tempting to attribute this low threshold simply to the high aspect ratio of the conductive filler. However, such a low value can only be explained in the light of a complicated dispersion and reaggregation behaviour during processing; in essence, well-dispersed nanotubes are destabilised and trapped just as a network forms [122]. The network formation behaviour can be manipulated not only by temperature and shear rate, but also by the application of external electrical fields [123], an approach that offers the possibility of achieving bulk conductive nanotube-polymer composites with anisotropic electrical properties, whilst maintaining a high degree of optical transparency.

In contrast, the thermal conductivity of cured nanotube-epoxy composites shows a minimal, or at best linear, increase with nanotube content. The enhancement appears to be greater for SWCNTs than CNFs [124], probably reflecting the intrinsic properties of the fillers, although it is impossible to rule out the effects of specific surface area and chemistry. In contrast to the electrical percolation behaviour, which is dominated by the filler network structure, the thermal conductivity of a composite is more sensitive to the quality of the interfacial bonding between filler and matrix. Whereas electrons travel along filler particles and can tunnel through remaining polymer barriers, thermally-activated phonons must be coupled into the polymer by a strong interface of intermediate thermal impedance. Even CNF loadings up to 40 wt% only lead to a moderate and linear increase in thermal conductivity of epoxy [112] and phenolic composites [113], as a function of filler content.

As an alternative to simple shear-mixing, MWCNTs can be introduced into more complex thermosetting composites by carrying them on the surface of a more conventional reinforcement. For example, MWCNTs can be grown on a stainless steel mesh for subsequent reinforcement of epoxy [125]. The resulting increase in surface area significantly increased the adhesion between the metal and the polymer. Such a volumetrically distributed interface as compared to a thin boundary layer may lead to an improved microcrack resistance. A similar effect has also been shown for catalytically-grown MWCNTs [126] and CNFs [127] on carbon fibre surfaces. Although the macroscopic fibre surface was somewhat damaged at the high temperatures used for the

nanotube/nanofibre growth, single fibre fragmentation tests showed reduced fragment lengths for the coated carbon fibres compared to the as-received fibres in epoxies, implying an improvement of interfacial shear strength of up to 500%.

3.2. Elastomeric carbon nanotube/nanofibre composites

Surprisingly little effort has been directed towards using nanotubes and/or nanofibres as a reinforcement in elastomeric polymers. A comparative study on silicone-based nano-composites containing bundles of SWCNTs and CNFs has been reported by Frogley *et al.* [128]. Filler loading fractions of 1 and 4 wt%, respectively, were achieved. An evaluation of the mechanical tensile properties showed an approximately linear increase in composite stiffness, but also a reduction in strength and strain to failure for both types of filler, with increasing loading fraction. The increase in initial modulus (a linear stress-strain behaviour up to an elongation of 10% was assumed) was more pronounced for the bundles of SWCNTs compared to the nanofibres, although the (modest) CNF composite stiffnesses compare well with data for similar nanofibres in a rubbery epoxy [129]. However, at a higher strain, around 80%, the stiffness of the rubber composites was found to be similar, within experimental accuracy, independent of filler type and loading fraction. On the other hand, the addition of up to 10 wt% CNFs in rubbery epoxy did lead to a significant increase in composite strength and strain to failure [129]. Such increases in properties are not observed for comparable loading fractions of spherical carbon black particles in the same matrix, highlighting the influence of an increased aspect ratio. Catalytically-grown MWCNTs dramatically increased the modulus and strength of a similar flexible epoxy, but reduced the strain to failure at a loading of 4 wt% [117]. These differences in composite performance most likely reflect variations in the quality of the filler dispersion, since the entangled MWCNTs formed clusters which reduced the deformability of the composite. In general, the nanofillers have proportionately greater influence on the stiffness of rubbery matrices than hard ones, due to the lower intrinsic modulus.

The stiffness of elastomeric composites generally depends on the distribution of particles, whereas the dispersion is critical for the strength and strain to failure [130]. Fundamental issues regarding the matrix chemistry, especially the degree of cross-linking as a function of nanotube type and loading fraction, as well as the direct interfacial strength have not yet been established. However, it is well known that the surface area surface chemistry of carbon black has a pronounced influence on the resulting properties of elastomeric nanocomposites [131,132] and some similar effects may be anticipated.

3.3. Thermoplastic carbon nanotube/nanofibre composites

Approaches to the manufacture of nanotube/nanofibre thermoplastic composites cover a very broad range of processing technologies, including, in some cases, combinations of different methods. Standard techniques such as extrusion and injection-moulding are preferred for economical reasons, but are often inapplicable due to limited quantities of nanofiller or the desire for high volume fractions. A concise review of the literature poses some difficulties due to the vast number of experimental parameters that have been explored. The studies, although mostly consistent in themselves, generally evaluate rather different composite systems and seldom present both an assessment of mechanical performance and matrix morphology. Thus, a complete, consistent picture has not yet emerged.

3.3.1. Thermoplastic nanotube/nanofibre composites processing: dispersion and alignment

Composite processing machines ranging from bench-top, custom-made injection-moulding machines, suitable for small-volume composites, to large-scale extruders have been used to produce nanotube/nanofibre-filled compounds. In general, straightforward addition of nanotube/polymer mixtures to processing machines is complicated by the low apparent density (typically around 0.1 g cm^{-3}) of as-produced filler materials. Both solution- and dry-blending of the nanotube-polymer components have been used prior to the extrusion step [133–135]. In

addition, this type of initial solution-compounding can lead to polymer-coated nanotubes, which may assist subsequent dispersion in other thermoplastic matrices [136].

Substantial shear forces appear to be necessary during the first composite processing step, in order to disperse nanotubes and nanofibres in the polymer, especially in the as-produced state and at high filler loadings. For example, filler contents up to 60 wt% of nanofibres [137] and about 30 wt% of MWCNTs [138] in thermoplastics have been realised using melt-compounding. In the case of nanotubes especially, the degree of nanotube dispersion depends on both the entanglement state of the as-received material and the particular processing technology. In general, the degree of dispersion is reasonable in thermoplastic systems, and better than in thermosets. As an example, Figure 7 shows the dispersion of commercial carbon nanofibres in a thermoplastic poly(ether ether ketone) (PEEK) matrix as a result of twin-screw extrusion at a nanofibre loading fraction of 15 wt%. The high intrinsic viscosity of thermoplastic matrices in general, has the dual advantage of

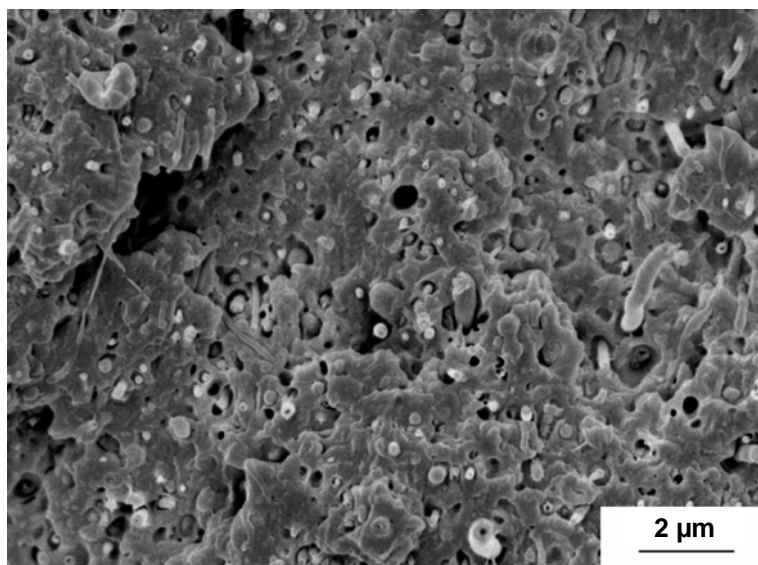


Fig. 7. Representative scanning electron micrograph showing dispersed carbon nanofibres in a poly(ether ether ketone) matrix at a filler content of 15 wt% after twin-screw extrusion.

increasing the shear applied to the aggregates (even breaking the individual CNTs/CNFs) and minimising the opportunity for reaggregation. However, even extensive twin-screw extrusion does not lead to a complete break-up of the entanglements in commercially available catalytically-grown MWCNTs [139–141]; nanotube clusters are observed even at low filler concentrations. Prolonged mixing times simply lead to an improved distribution of nanotube aggregates [140]. In contrast, nanotube weight fractions of up to 30 wt% of arc-grown as well as of CVD-grown MWCNTs were shown to disperse in poly(methyl methacrylate) (PMMA) [138] and polystyrene (PS) [135] matrices, and the use of aligned, rather than entangled CVD nanotubes, also appears to be advantageous [142]. Although filler dispersion can be aided by ball milling of the raw filler material prior to processing [143], this approach degrades the aspect ratio of individual particles significantly more than shear-intensive melt processing [144].

Interestingly, nanofibre loading fractions up to 10 wt% were found to have no significant influence on the shear viscosity of polypropylene (PP) composites in the shear rate regime typically encountered during thermoplastic processing [145]. In case of a polycarbonate (PC) matrix, the shear viscosity was even reduced with increasing nanofibre content up to 10 wt% [146], most likely as a result of pronounced shear alignment of the filler, a well known behaviour for short fibre-filled polymers [147]. At higher nanofibre loadings, however, the rheological behaviour of such polymer nanocomposites changes. A pronounced increase in shear viscosity, especially at low shear rates, reflects the presence of a nanofibre network structure and/or aggregates [145]. Similar rheological thresholds were observed for oxidised CNFs, at even lower loadings, indicating a greater interfacial interaction during processing [146,148] and for compounds based on entangled MWCNTs [139]. This rheological threshold depends on the nanotube/nanofibre type and treatment as well as on the polymer matrix and generally indicates the onset of interactions between individual filler particles or clusters.

In addition to melt-processing, significant efforts have been made to cast nanotube-thermoplastic polymer films directly from solution. However, most systems require large volumes of solvents in order to fully solubilise both the polymer and then the nanotubes. Common

solvents are organic liquids of high toxicity such as toluene, chloroform, tetrahydrofuran (THF), or dimethyl formamide (DMF), although a number of aqueous systems have also been explored. Solution-casting has been used to manufacture MWCNT-containing PS [149–151], poly(hydroxyaminoether) (PHAE) [152,153], poly(vinyl alcohol) (PVA) [106,154], ultra-high molecular weight polyethylene (UHMWPE) [155] and PP [156] composite films with homogeneous nanotube dispersions. Similarly, SWCNT-containing PP [157], PVA [158,159] and PVA/PVP (poly(vinyl pyrrolidone)) [160] composite films have been prepared. In many cases, ultrasonication is used to aid nanotube dispersion in the liquid state, although prolonged high-energy sonication has the potential to introduce defects into nanotubes [161]; the ultrasonic treatment may also stabilise the dispersion by grafting polymer onto the CNT surface through trapping of radicals generated as a result of chain scission [162]. In addition, surfactants [160,163], polymer-functionalised nanotubes [158,164], and other chemical treatments of the constituents [165] are often employed. Last but not least, a number of studies have investigated the creation of nanotube-polymer composites [166–170] by *in-situ* polymerisation.

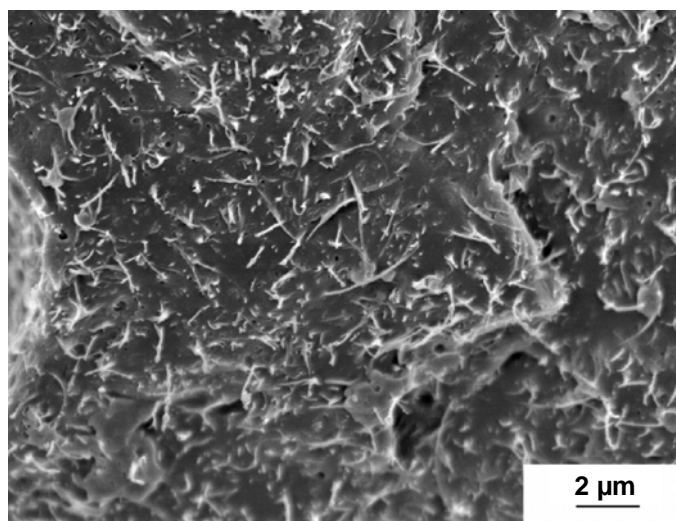


Fig. 8. Representative scanning electron micrograph showing dispersion of 5 wt% of CVD-grown MWCNTs in solution-cast and subsequently hot-pressed polypropylene.

The quality of the nanotube/nanofibre dispersion appears to strongly depend on the initial degree of entanglement of the as-prepared materials, as well as on the strength of the shear forces experienced during processing. Ideally, the individual nanotubes should form an inherently electrostatically or sterically stabilised dispersion, with a long lifetime relative to the casting process. The nature of the interaction between nanofiller and polymer is particularly important in relatively low viscosity solutions in which reaggregation can be rapid. A range of amphiphilic, water-soluble polymers have been found to solubilise SWCNTs efficiently in aqueous solution [171], effectively acting as surfactants. Alternatively, CNTs can be functionalised in order to produce stable dispersions in the desired solvent; for example, oxidation produces electrostatically-stabilised MWCNTs in water [101]. Once the solvent is removed, and the nanofillers are homogeneously dispersed, subsequent sample processing does not necessarily require shear forces. For example, the dispersion can be maintained during subsequent compression-moulding of solution-blended material [135,138,144]; the comparatively high melt viscosity of thermoplastics, as compared to epoxies for example, appears sufficient to prevent reaggregation of the filler. Figure 8 demonstrates that a good dispersion can be retained in a system of 5 wt% CVD-grown MWCNTs in polypropylene processed by solution-casting and subsequent hot-pressing.

Processing of compounds under conditions involving both shear and elongational flows, such as injection-moulding, can be used to induce alignment of the nanofiller [172]. Similarly, Kuriger *et al.* showed that flow-induced nanofibre alignment occurred during extrusion [144]; the degree of nanofibre alignment was improved by optimisation of the extruder die geometry. Keeping the extruded strand under tension minimised die swell effects and the orientation of the filler was maintained. However, a decreasing degree of alignment with increasing nanofibre content was observed, most likely as a result of nanofibre-nanofibre interactions altering the flow field [144]. Similarly, drawing of composite extrudates was shown to induce significant nanotube alignment [135] as did mechanical stretching of solid nanocomposites above the glass transition temperature [152,153], spin-casting of

nanotube-polymer solutions [151], and the application of magnetic fields during *in-situ* polymerisation [173].

In addition, a number of studies have investigated the direct melt-spinning of composite fibres [142,174–181]. Similar to hot-drawing of nanocomposites [152], such melt-spinning leads to an improved alignment of the nanoscale filler and the polymer matrix, thereby maximising composite performance. As shown in Figure 9 for a melt-spun polyamide-12 nanocomposite fibre containing 5 wt% of CVD-grown MWCNTs, such melt-spinning leads to aligned nanotubes in the polymer fibre while maintaining a good quality of the overall fibre surface finish. In the case of SWCNT bundles in an isotropic petroleum pitch matrix, a pronounced influence of the filler on the melt elongation behaviour of the composite was observed [174]. Such an increase in melt elongation properties, with nanotube addition, enhances the spinnability of polymers. For example, fine CNF-polyester (PET) fibres with diameters as low as 25 μm can be produced under stable conditions [178]. Measurements of the extensional rheology of PEEK/CNF blends have quantitatively demonstrated improvements in extensional viscosity and melt strength, and have shown that the resulting stabilisation of the melt allows the production of novel PEEK foams [182]. In fact, as shown in Figure 10, at high elongation shear rates, there is a crossover leading to reduced viscosity, but at rates relating to foaming processes [183],

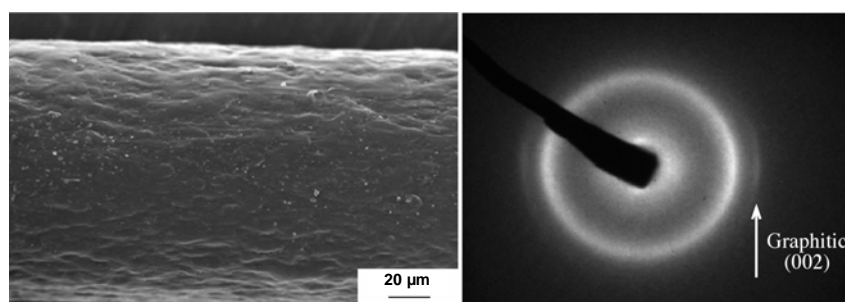


Fig. 9. Scanning electron micrograph of surface finish of melt-spun polyamide-12 nanocomposite fibre containing 5 wt% of CVD-grown MWCNTs and the corresponding 2D WAXS fibre diffraction pattern highlighting the nanotube alignment (evidenced by the anisotropic arc in the graphitic (002) peak arising from the intershell spacing).

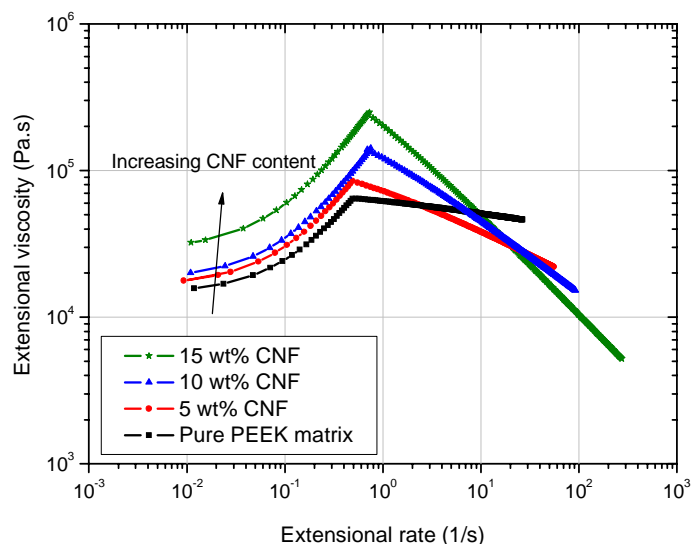


Fig. 10. Apparent elongational viscosity of a PEEK matrix at 360°C as a function of the strain rate with increasing nanofibre content as determined by uniaxial Rheotens melt elongation experiments.

bubble expansion is stabilised. Carbon nanostructures can thus beneficially alter the processing behaviour of polymers, as well as enhancing the properties of the resulting composite solids [184].

In addition to melt processing, solution-spinning has also been successfully used to produce high loading fraction SWCNT-PVA fibres. Surfactant-stabilised dispersions of CNTs are injected into a PVA bath, forming a fibre that can be handled and drawn [185,186]. There is a desire to exploit lyotropic liquid crystalline phases to produce fibres with improved alignment. Some promising steps have been taken in this direction using pure CNT dispersions [187,188], as well as combinations of SWCNTs with the rigid rod polymer PBO [167]. Solution-processing has also been used to produce composite films using a Layer-By-Layer technique to deposit alternating thin layers of negatively charged SWCNTs and positively charged polyelectrolyte [189].

3.3.2. Mechanical properties of thermoplastic nanotube/nanofibre composites

The published mechanical data show that the tensile modulus of nanotube/nanofibre-thermoplastic composites is generally improved, although a detailed comparison of the data is difficult due to the different types of fillers, surface treatments, matrices, processing techniques, and test methods that have been used. In general, the stiffening effect of nanotubes and nanofibres appears to be more prominent in semicrystalline rather than amorphous thermoplastics, possibly due to the nucleation effects discussed below. Although a linearly increasing composite stiffness has been observed up to 15 wt% of nanofibres [172], in many cases, a non-linear relationship is observed with increasing filler loading fraction. Even when a homogeneous dispersion of the nanoscale filler is claimed for all concentrations, the stiffness enhancement is usually most prominent for low filler weight fractions, with the critical concentration depending on the specific materials and processing conditions used. This observation might relate to the decreasing nanofiller alignment with increasing weight fraction [144,151], although alignment variations of the polymer matrix have not properly been taken into account. In semicrystalline matrices the (often unanalysed) increases in crystallinity may be the source of the non-linearity. Furthermore, in most cases, there are probably changes in dispersion (which are notoriously hard to quantify), as the larger surface areas associated with high loading fractions become increasingly difficult to accommodate within the polymer; similar effects have been seen in nanoclay-filled polymers [190]. However, even in the presence of nanotube clusters, enhancements in composite stiffness can be observed [134]. Overall, some interesting trends in composite stiffness can be distinguished. For example, Figure 11 shows a comparative plot of the tensile modulus of melt-compounded nanofibre-reinforced (a) amorphous PC [146] and PMMA [133], and (b) semicrystalline PP [143,144,191] and PEEK [192] composites as a function of reported nanofibre weight and volume fraction, respectively.

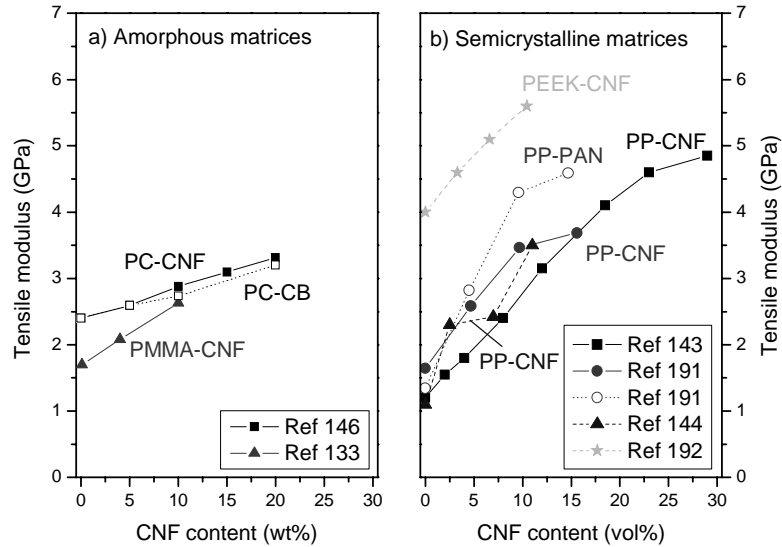


Fig. 11. Comparative evaluation of composite stiffness increase for nanofibre-reinforced (a) amorphous and (b) semicrystalline matrices as a function of nanofibre loading.

Considering the case of the amorphous matrices, in Figure 11a, both studies revealed a linear increase in composite stiffness with increasing nanofibre weight fraction. A good dispersion of nanofibres was claimed [133,146], independent of filler weight content. Furthermore, partial nanofibre alignment in the direction of the tensile axis can be assumed as a result of the shear flow conditions during production, and was verified by extensive image analysis of TEM images in the case of the PMMA composites [133]. More disappointingly, comparable PC composites containing dispersed equiaxed carbon black particles showed an identical increase in composite tensile modulus to the CNF composites [146]. The relative increase in composite tensile modulus with increasing nanofibre content is only slightly higher for the PMMA composites but agrees well with other data for melt-spun composite fibres [180]. Turning to the melt-compounded, semicrystalline, PP nanocomposites shown in Figure 11b, more pronounced increases in composite tensile stiffness, with the addition of nanofibres, are apparent, as compared to the amorphous composites. This increase is linear only up to a critical

nanofibre volume fraction which varies between the studies. A direct comparison to values for short PAN-based carbon fibres in PP (processed under similar conditions) indicates a smaller reinforcement for the nanofibres. In the case of the PEEK data, the increase in stiffness is linear (a constant degree of crystallinity was confirmed); the slope can be used to extract a modulus of the CNFs if a simple short fibre model is assumed and if the aspect ratio and orientation are known [172]. Experimentally, these factors are hard to establish accurately, but estimates put the CNF tensile modulus at around 100 GPa, lower than that of CNTs grown at high temperature but consistent with expectations for CVD-grown CNFs.

Comparable loading fractions of MWCNTs, rather than CNFs, in both solution-cast [149,151] and extruded PS films, produced a more pronounced stiffness enhancement, indicating that the crystalline quality of the nanoscale filler contributes to the overall performance of the nanocomposite. Similarly, comparisons of different types of filler in PA-12 composite fibres showed that well-dispersed CNTs produce a greater improvement in stiffness than CNFs, but that the type of nanotube also has an effect [142]. In addition, a direct comparison of aligned versus unoriented nanotubes showed a significant enhancement of the composite stiffness for the aligned nanotubes [135].

Dynamic mechanical testing as a function temperature has shown that the stiffening effect of the nanotubes is more pronounced above the softening point of the matrix, in both MWCNT-PMMA [138] and MWCNT-PVOH [106] composites. In addition, the glass transition temperature is often increased. This observation indicates that the matrix mobility is influenced by the presence of the nanotubes, a common effect for polymer systems containing finely dispersed particles [193].

Turning to other mechanical properties, enhancements in composite yield stress, strength, and toughness generally appear more difficult to achieve, especially for filler loading fractions exceeding about 10 wt%. Improvements in impact strength of nanofibre and nanotube-reinforced PMMA composites [133] and in tensile strength of amorphous MWCNT-PS nanocomposites [135,149,151] have been reported. These properties depend on the homogeneity of specimens achieved during processing as well as on interfacial issues relating to the specific filler

types and matrices. For example, the impact properties of nanofibre-PC composites were significantly decreased, even at low nanofibre contents, most likely as a result of aromatic hydrocarbons on the nanofibre surface enhancing chemical stress cracking of the polycarbonate [146]. The most prominent strength enhancements of bulk nanocomposites have been achieved for well-dispersed and aligned nanofibres in PEEK [172], up to filler loading fractions of 10 vol%, and in PP [144], at nanofibre loading fractions as low as 5 vol%. In the PP case, a further sub-linear strength increase up to 11 vol% CNFs was reported. This deviation from a linear relationship most likely reflects the decreasing nanofibre alignment at higher filler contents, but might also be a consequence of microstructural variations and an increasing void content at higher concentrations [112]. Improvements in yield strength have also been reported in a number of nanocomposite fibre systems, as discussed later.

CNTs and CNFs are also interesting additives for tribological applications [194]; they can significantly reduce the wear rate of polymers, apparently independently of the degree of nanotube dispersion achieved during processing. Although the exact wear reducing mechanism of the nanoscale constituent is as yet not clear, there appear to be number of beneficial effects contributing to the overall performance increase. Firstly, the basic strength and stiffness of the nanocomposites is enhanced; secondly, the small size of the nanomaterials results in smaller wear debris particles and therefore less pronounced roughening of the bearing counterparts; thirdly, the carbon-based fillers may act, or break up to act, as solid lubricants under dry sliding conditions. These nanoscale fillers can be easily compounded together with standard, more established tribological aids (such as PTFE or carbon fibres), to allow fine-tuning of the resulting overall mechanical performance. As an example, the observed improvements in specific wear rate of a range of commercial high-performance PEEK compounds with the addition of 10 wt% of carbon nanofibres are shown in Figure 12. The wear-reducing potential of carbon nanostructures is currently being studied in a range of ultra-high molecular weight polyethylene composites for medical joint replacement applications [195]. In addition, of course, the nanofillers provide the means to improve the wear

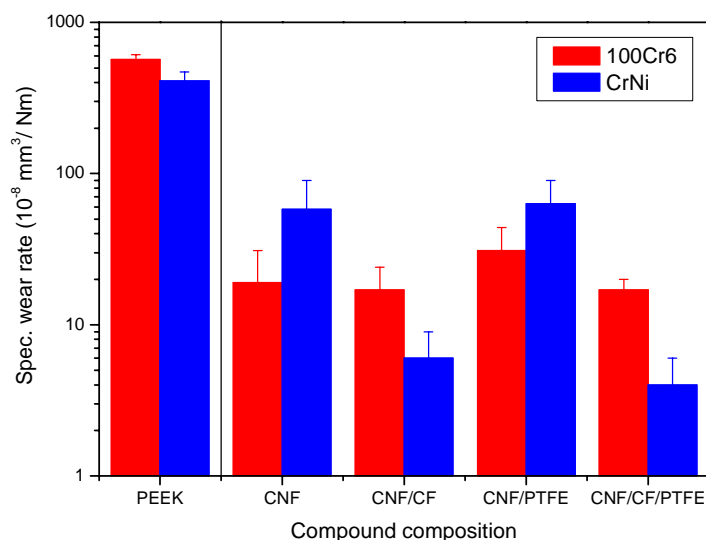


Fig. 12. Influence of a 10 wt% carbon nanofibre loading on the wear performance of a PEEK matrix and a range of commercial PEEK compounds for tribological applications against two different steels.

properties of microstructured parts in which more conventional fillers cannot be accommodated, and in which problems of erosion are particularly problematic. As an example, Endo and colleagues helped Seiko develop a CNF-filled nylon watch gear, less than 200 μm in diameter.

A number of studies have shown a significant influence of the nanoscale fillers on the resulting morphology of a semicrystalline matrix. The microstructure, in terms of crystal structure, crystallinity, and crystal orientation, of a semicrystalline polymer is dependent on its thermal history, the manufacturing process employed, and the presence of possible nucleation sites. The combination of high shear and elongational flows, occurring during processing under non-isothermal conditions, leads to complex variations in molecular orientation and crystal morphology. Furthermore, there is a direct influence of reinforcing fibres on the surrounding matrix which depends on the interfacial interactions,

the fibre volume fraction, as well as the aspect ratio and orientation of the fibres [196,197]. Finally, relative movements between filler and matrix during processing result in a modification of the local flow field and molecular conformation. In the case of PP, nanofibres [137,198], MWCNTs [156,198], and SWCNTs [157,179,199] were all found to alter the crystallisation kinetics and the resulting crystal structure in terms of average crystal size and degree of crystallinity. Similar nucleation effects have been observed for carbon black [200] and nanoclays [201] in semicrystalline PP. In addition, SWCNTs were shown to induce polymorphism in PP [157] and to alter the proportions of the polymorphs in PVDF [202]. Direct evidence for such variations in matrix morphology is shown in Figure 13; transmission microscopy highlights the clear variation in molecular arrangement in the vicinity of nanofibres in highly oriented polypropylene drawn from solution [198].

Microstructural development is even more important for highly oriented polymers, such as melt-spun fibres. There are two important deformation processes which govern the resulting mechanical and physical properties of melt-spun thermoplastic fibres: melt- drawing and subsequent drawing in the solid state. The final orientation of polymer molecules depends on the relative draw ratios applied during the two process stages [203] and such orientations influence the crystallization kinetics [204]. Filler particles acting as nucleation sites can further alter

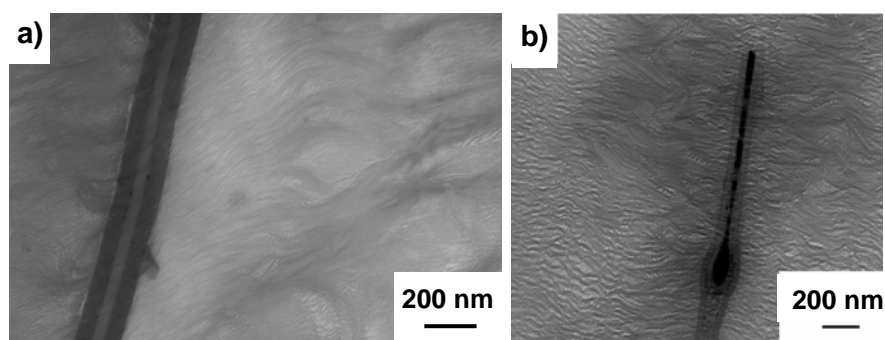


Fig. 13. Transmission electron micrographs of variations in local polymer crystallinity in the vicinity of nanofibres in highly oriented PP, drawn from solution (with permission from [198]). In (a) note the debonded interface on the left, and the associated lack of matrix modification.

the structural development [204]. One would therefore expect nanofibres and nanotubes to have a pronounced effect on the microstructure of spun composite fibres. Such effects are likely to prove even more prominent than those observed for colouring pigments and common nucleating agents such as talc [205], since the high aspect ratio of dispersed nanotubes and nanofibres could lead to a significant load transfer in the molten state, as observed experimentally [174,182].

Melt-spinning of nanofibre-reinforced PP composite fibres significantly improved the relative modulus increase, most likely as a result of enhanced nanofibre alignment [175,176]. This improvement strongly depended on the draw ratio of the composite fibres and on the filler content [175]. Increasing the CNF content above 5 vol% did not further increase the composite modulus at higher draw ratios, as in the case of amorphous polymer composite fibres. On the other hand, the initial stiffening effect of small additions of SWCNTs to PP fibres dwarfs the impact of CNFs but appears to saturate at loading fractions as low as 1–2 wt% [177]. The greater impact of the SWCNTs may be attributed to their intrinsically greater perfection and their flexibility which may allow them to align better during processing. The saturation effect is not yet fully understood, although, again, it may relate to the difficulty of accommodating the very high surface area of SWCNTs. On the other hand, the possible microstructural variations were not considered and initial increases in crystallinity, due to nucleation effects, might contribute to the rapid improvements in composite stiffness. In contrast, a modest stiffening effect but a large increase in nanocomposite strength and toughness has been reported for entangled MWCNTs in UHMWPE films [155]. The toughness of these nanocomposites was further improved by a subsequent drawing process at elevated temperatures which led to an increased ductility compared to the pure polymer. Here, electron microscopy provided direct evidence for nanotube-nucleated shish-kebab PE crystals, an effect that might account for the observed ductility improvement in these semicrystalline nanocomposites. Attempts to improve the performance of existing high performance fibres has met with mixed success, but the introduction of SWCNTs into PBO has been shown to improve both stiffness and especially strength (by 50%), demonstrating that nanotubes do

have the potential to extend the ultimate mechanical performance of materials [167].

Some of the other most promising improvements in mechanical properties have appeared in solution-processed PVA nanocomposite fibres [185,186] which contain high loading fractions of SWCNTs, up to 60 wt%. The strength and stiffness of these fibres, of around 1 GPa and 100 GPa, respectively, are relatively high, although still modest compared to carbon fibres (and theoretical predictions); however, the strain to failure can be large, leading to a very high-energy absorption; Figure 14 shows that the combined strength and strain to failure of these fibres lies outside the envelope of conventional materials. Similar, basic fibre properties have been obtained from pure SWCNT fibres, either as-grown [206] or spun from a lyotropic superacid solution [188]. There is still plenty of scope for improving the alignment and density of nanotubes within these fibres. The Layer-By-Layer assembly of SWCNT films produced a 2D tensile strength of 220 MPa, comparing favourably with engineering ceramics [189].

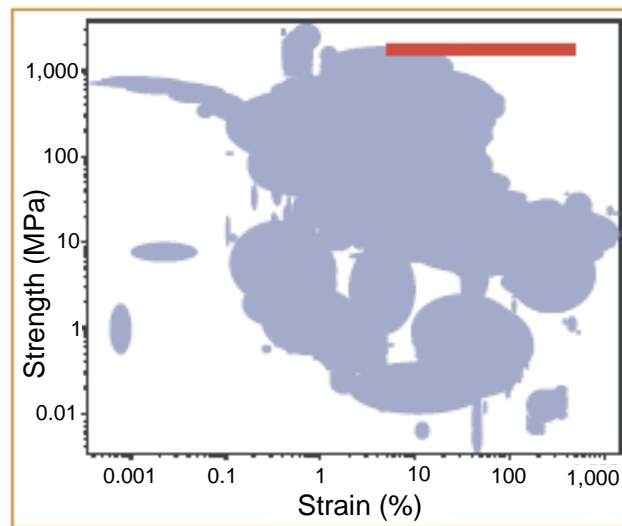


Fig. 14. Comparison of the strength and failure strain for carbon nanotube composite fibres for different degrees of initial pre-draw (red line) and the 3,000 materials of all types (grey field) in the Cambridge Materials Selector database. Taken from [186].

3.3.3. Transport properties of thermoplastic nanotube/nanofibre composites

As well as mechanical reinforcement, there is considerable interest in functional nanocomposites in order to exploit the unique physical properties, such as high thermal or electrical conductivity, of the constituents. Electrically conductive polymer composites, for example, are used in anti-static packaging applications, as well as in specialised components in the electronics, automotive, and aerospace sector. The incorporation of conductive filler particles into an insulating polymer host leads to bulk conductivities at least exceeding the anti-static limit of 10^{-6} S/m. Common conductive fillers are metallic or graphitic particles in any shape (spherical, platelet-like or fibrous) and size. However, the incorporation of CNTs allows for a low percolation threshold, a high quality surface finish, a robust network, and good mechanical properties – a combination not obtained with any other filler. The use of CNTs/CNFs as a conductive filler in thermoplastics is their biggest current application, and is widespread across the automotive and electronic sectors.

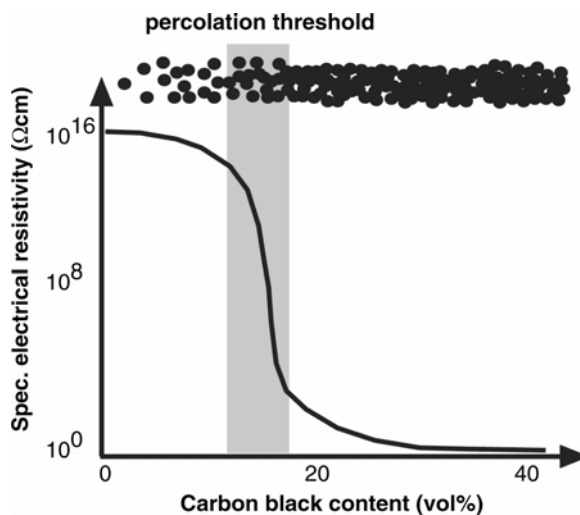


Fig. 15. Schematic representation of the electrical resistivity in a carbon black-filled functional polymer composite with increasing filler loading fraction (according to [207]).

In general, the electrical conductivity of a particulate composite reveals a non-linear increase with the filler concentration, passing through a percolation threshold, as shown in Figure 15. At low filler concentrations, the conductive particles are separated from each other and the electrical properties of the composite are dominated by the matrix. With increasing filler concentration local clusters of particles are formed. At the percolation threshold, ϕ_c , these clusters form a connected three-dimensional network through the component, resulting in a jump in the electrical conductivity.

Close to the percolation threshold, the electrical conductivity follows a power-law of the form

$$\sigma_0 \propto (\phi_V - \phi_c)^t \quad \phi_V > \phi_c, \quad (2)$$

where ϕ_V is the volume fraction of the filler [208]. The exponent t in this equation was found to be surprisingly uniform for systems of the same dimensionality. For three-dimensional percolating systems t varies between 1.6 and 2, in simulations [209,210]. The percolation threshold is reduced on increasing the aspect ratio [211], but the maximum conductivity is limited by the contact resistance between neighbouring particles [212]. A related percolation behaviour is observed in the rheological properties, at the point when the filler particles begin to interact. In many cases, the electrical percolation threshold of bulk composites corresponds to the rheological threshold [139,141].

The electrical properties of nanofibre-thermoplastic composites exhibit characteristic percolation behaviour [145,213,214]. In the case of untreated CNFs, the critical volume fraction is between 5 and 10 vol%, but depends on the processing technique and resulting degree of CNF dispersion and alignment. At a higher filler content of 15 vol%, even drawing of nanofibre-filled PP composite fibres does not destroy the conductive network [gordeyev01]. However, a comparative study of bulk injection-moulded nanofibre and PAN-based short carbon fibre-PP composites showed a lower percolation threshold and a higher maximum bulk conductivity for the macroscopic filler [175].

The electrical properties of CNF-composites are influenced by surface and thermal treatments [214]. Oxidation increased the percolation threshold and decreased the maximum bulk conductivity, whereas high-temperature graphitisation produced the opposite trends. These results verify that the electrical performance of the composite depends on the intrinsic conductivity as well as the dispersion and alignment of the filler. Oxidation encourages interaction with the polymer, increasing the contact resistance, whereas graphitisation both reduces polymer interactions and improves the intrinsic conductivity. As an alternative to graphitisation, electro-deposition of copper on nanofibre surfaces has been shown to improve the maximum bulk composite conductivity [148].

Similarly, the electrical percolation threshold of thin MWCNT-thermoplastic films also depends on the type of nanotube and surface treatment. Threshold values from around 5 wt% for oxidised catalytic MWCNTs in PVA [106] to around 0.06 wt% and 0.5 wt% for arc-discharge MWCNTs in PVA [215] and PMMA [216], respectively, have been reported. Interestingly, the optical transparency of such conductive thin film composites for anti-static applications can be significantly improved by using SWCNTs [169], even in bundled form. As discussed previously for epoxy systems, these very low percolation thresholds are far below the expected values for randomly distributed fibres, and are the result of active aggregation processes.

A significant reduction in the critical nanotube volume fraction for electrical percolation can be achieved by exploiting the concept of double percolation through the formation of a co-continuous morphology in nanotube-filled polymer blends [141,217,218]. This concept of double percolation was introduced by Sumita *et al.* [219] who achieved percolation of carbon black in the continuous phase of a polymer blend. Similar success has been demonstrated for nanofibres in a PE/PMMA blend [220].

As in the case of the thermosetting systems, the thermal conductivity of nanofibre-thermoplastic composites does not show a percolation transition, even at higher filler volume fractions [112,144,213]. A linear increase in thermal conductivity is observed, although the magnitude depends to some extent on the alignment of the filler [144], in agreement

with data for short carbon fibre composites [221]. The overall performance increase for nanofibres was similar to that observed for short carbon fibres in a similar system [213].

4. Conclusions

Although commercial nanotube-polymer composites exist today, they almost exclusively employ relatively low loadings (3–5 wt%) within thermoplastic matrices for the purposes of anti-static dissipation, particularly in the automotive and electronics industries [222]. Such applications exploit bulk quantities of relatively defective catalytically-grown materials. On the other hand, individual perfect nanotubes appear to have axial stiffnesses towards that of diamond, and strengths ten times that of any other available material. There are, therefore, considerable efforts underway to exploit these properties in macroscopic structural composites. In addition to these remarkable headline mechanical properties, there is interest in thermal conductivity, thermal stability, flame retardance, wear resistance, and so on. However, the successful exploitation of the promising mechanical and other properties of CNTs and CNFs in polymer composites is as yet hindered by a number of fundamental issues.

It has become clear that issues of dispersion, alignment, and stress transfer are crucial, and often problematic at this size scale. Dispersion is often obtained by using unentangled nanotubes, high viscosities, and high shear rates. However, a more subtle approach uses surface modifications or coatings on the nanofiller to stabilise individual particles. Surface modification has the added advantage of improving stress transfer to the matrix (although it tends to increase contact resistance). The drawback with the direct modification of the filler surface is that it will damage the properties of SWCNTs and the outer shell(s) of MWCNTs. The area of surface chemistry of nanotubes is therefore an important area for future development. A degree of alignment has been successfully obtained using shear and elongation, as well as, to a lesser extent, magnetic and electrical fields. However, as with the development of high-performance polymers, producing materials that approach perfect orientation will be challenging.

One major uncertainty is the type and quality of nanotubes that should be used. A wide variety of synthesis methods have been employed, yielding nanotubes of different size, aspect ratio, crystallinity, crystalline orientation, purity, entanglement, and straightness. All these factors affect the processing and properties of the resulting composites but it has not yet emerged what the 'ideal' carbon nanotube would be; the answer may vary with the matrix and application. As an example, consider even the question of the ideal nanotube diameter. Very small diameters, particularly single-wall nanotubes, are relatively flexible, potentially leading to lower viscosities and greater robustness during processing, but also to potentially persistent entanglements. The higher the surface area, the greater the impact of the nanotubes on matrix conformation and crystallinity; the nature and significance of such effects are not yet clear but depend on the polymer used. For the smallest nanotube sizes, where the diameters of the nanotubes and polymer molecules are similar, particulate concepts from composite or nucleation theory may no longer be helpful. The composite is essentially a polymer-polymer blend, although one with rather unusual characteristics which may give rise to new behaviours.

One major difficulty with small diameter nanotubes is that they become increasingly difficult to wet. By trivial estimation, even a 1 vol% loading of single-wall nanotubes ensures that all of the polymer molecules are within one radius of gyration (say 5 nm) of a nanotube. This result implies that a complete wetting of high loading fractions of single-wall nanotubes will be difficult, at least by conventional means, and that even more modest concentrations may be brittle and hard to process due to the constraint of the matrix. Alternative approaches, based on layer-by-layer assembly and possibly lyotropic spinning of single-wall nanotube solutions have already been explored and proven to be interesting routes to thin films and fibres. However, for the purpose of simple, bulk composites, intrinsically straight, highly crystalline, multi-wall nanotubes might be expected to yield the best mechanical properties, as long as internal shear failures can be minimised. It remains to be seen whether there is an optimal defect concentration that prevents internal sliding without harming the intrinsic properties excessively. Strain arguments would suggest that smaller multi-wall nanotubes will

be less prone to shear failure than their larger relatives. When taken together with the supposed greater perfection of higher curvature nanotubes due to self-selection during growth, it might be hypothesised that small diameter multi-wall nanotubes, with say 2–4 shells, should be preferred.

5. Outlook

Whichever type of nanotube is selected, it will be necessary to develop new synthesis routes. At present, catalytic MWCNTs and CNFs appear as the optimum choice, given that such materials can be most readily obtained in large quantities with a high purity. However, these materials are intrinsically defective and wavy, both of which are expected to be highly detrimental to the mechanical performance [223]. Somehow nanotubes with a crystalline quality closer to arc-grown nanotubes need to be obtained at a cost similar, or indeed below, current CVD-grown products.

As the absolute size of the reinforcement decreases towards the size of the polymer molecules, interactions between filler and matrix become more important, both during processing as well as in the solid-state. Significant progress has been made in understanding the interactions between polymers and flat surfaces, but the interactions of polymers with highly curved surfaces at the molecular scale, are still largely unknown. Variations in crystallinity are important but the effects of constraint and other changes in polymer morphology in the vicinity of highly curved surfaces may also have significant effects on the deformation behaviour of the composite. As in biological nanocomposites, a high strength might not be exclusively linked to the intrinsic strength of the filler but might reflect increased yield stresses in the vicinity of the filler, as recently observed during pull-out experiments [224]. Given these issues and the change in scale towards molecular dimensions, it is not surprising that concepts of traditional fibre-reinforced composites are often not applicable to nanocomposites. Further work is required to provide a sound theoretical basis which will allow the successful prediction of the resulting mechanical and physical properties of nanotube/nanofibre-based polymer composites.

Carbon nanotubes and nanofibres may not produce practical replacements for existing high-performance materials in the near future. However, there is continuing market for electrically conducting polymer compounds, and immediate potential to develop the reinforcement of delicate composite structures such as thin films, fibres, and the matrices of conventional fibre composites. Indeed, market projections for polymer nanocomposite technology show a 160 million lb market for carbon nanotube-filled products by 2009 [225]. Although the full potential of nanotube composites remains to be realised, much progress has been made, and these nanocomposite systems have a bright future once the fundamental questions are resolved.

References

1. P.M. Ajayan, P. Redlich, M. Rühle; "Structure of carbon nanotube-based nanocomposites", *J. Microsc.-Oxford* 185(2) (1997), 275–282.
2. H.J. Gao, B.H. Ji, I.L. Jäger, E. Arzt, P. Fratzl; "Materials become insensitive to flaws at nanoscale: Lessons from Nature", *Proc. Nat. Acad. Sci. USA* 100(10) (2003), 5997–5600.
3. L.T. Drzal, M.J. Rich, M.F. König, P.F. Lloyd; "Adhesion of graphite fibers to epoxy matrices. 2. The effect of fiber finish", *J. Adhesion* 16(2) (1983), 133–152.
4. S.H. Wu; "A generalized criterion for rubber toughening – the critical matrix ligament thickness", *J. Appl. Polym. Sci.* 35(2) (1988), 549–561.
5. A. Galeski; "Strength and toughness of crystalline polymer systems", *Prog. Polym. Sci.* 28(12) (2003), 1643–1699.
6. T. Ebbesen; "Carbon Nanotubes, Preparation and Properties", CRC Press USA (1997).
7. H.W. Kroto, J.R. Heath, S.C. O'Brian, R.F. Curl, R.E. Smalley; "C₆₀: Buckminsterfullerene", *Nature* 318(6042) (1985), 162–163.
8. W. Krätschmer, L.D. Lamb, K. Fostiropoulos, D.R. Huffman; "Solid C₆₀: A new form of carbon", *Nature* 347(6291) (1990), 354–358.
9. S. Iijima; "Helical microtubules of graphitic carbon", *Nature* 354(6348) (1991), 56–58.
10. A. Oberlin, M. Endo, T. Koyama; "Filamentous growth of carbon through benzene decomposition", *J. Cryst. Growth* 32(3) (1976), 335–349.
11. R. Bacon; "Growth, structure, and properties of graphite whiskers", *J. Appl. Phys.* 31(2) (1960), 283–290.
12. P.J.F. Harris; "Carbon nanotubes and related structures", Cambridge University Press (2001).
13. D.S. Bethune, C.H. Kiang, M.S. de Vries, G. Gorman, R. Savoy, J. Vazquez, R. Beyers; "Cobalt-catalysed growth of carbon nanotubes with single-atomic-layer walls", *Nature* 363(6430) (1993), 605–607.

14. C. Journet, W.K. Master, P. Bernier, A. Loiseau, M. Lamy de la Chapelle, S. Lefrant, P. Deniard, R. Lee, J.E. Fischer; "Large-scale production of single-walled carbon nanotubes by the electric-arc technique", *Nature* 388(6644) (1997), 756–758.
15. A. Thess, R. Lee, P. Nikolaev, H. Dai, P. Petit, J. Robert, C. Xu, Y.H. Lee, S.G. Kim, A.G. Rinzler, D.T. Colbert, G.E. Scuseria, D. Tomanek, J.E. Fischer, R.E. Smalley; "Crystalline ropes of metallic carbon nanotubes", *Science* 273(5274) (1996), 483–487.
16. H.M. Cheng, F. Li, G. Su, H.Y. Pan, L.L. He, X. Sun, M.S. Dresselhaus; "Large-scale and low-cost synthesis of single-walled carbon nanotubes by the catalytic pyrolysis of hydrocarbons", *Appl. Phys. Lett.* 72(25) (1998), 3282–3284.
17. J. Tersoff, R.S. Ruoff; "Structural properties of a carbon-nanotube crystal", *Phys. Rev. Lett.* 73(5) (1994), 676–679.
18. T.W. Ebbesen, P.M. Ajayan; "Large-scale synthesis of carbon nanotubes", *Nature* 358(6383) (1992), 220–222.
19. D.T. Colbert, J. Zhang, S.M. McClure, P. Nikolaev, Z. Chen, J.H. Hafner, D.W. Owens, P.G. Kotula, C.B. Carter, J.H. Weaver, A.G. Rinzler, R.E. Smalley; "Growth and sintering of fullerene nanotubes", *Science* 266(5188) (1994), 1218–1222.
20. M. Cadek, R. Murphy, B. McCarthy, A. Drury, B. Lahr, R.C. Barklie, M. in het Panhuis, J.N. Coleman, W.J. Blau; "Optimisation of the arc-discharge production of multi-walled carbon nanotubes", *Carbon* 40(6) (2002), 923–928.
21. A.G. Rinzler, J. Liu, H. Dai, P. Nikolaev, C.B. Huffman, F.J. Rodriguez-Macias, P.J. Boul, A.H. Lu, D. Heymann, D.T. Colbert, R.S. Lee, J.E. Fischer, A.M. Rao, P.C. Eklund, R.E. Smalley; "Large-scale purification of single-wall carbon nanotubes: Process, product, and characterization", *Appl. Phys. A* 67(1) (1998), 29–37.
22. M. Endo, K. Takeuchi, S. Igarashi, K. Kobori, M. Shiraishi, H.W. Kroto; "The production and structure of pyrolytic carbon nanotubes (PCNTs)", *J. Phys. Chem. Solids* 54(12) (1993), 1841–1848.
23. C.N.R. Rao, A. Govindaraj, R. Sen, B.C. Satishkumar; "Synthesis of multi-walled and single-walled nanotubes, aligned-nanotube bundles and nanorods by employing organometallic precursors", *Mater. Res. Innovat.* 2(3) (1998), 128–141.
24. R. Andrews, D. Jacques, A.M. Rao, F. Derbyshire, D. Qian, X. Fan, E.C. Dickey, J. Chen; "Continuous production of aligned carbon nanotubes: A step closer to commercial realization", *Chem. Phys. Lett.* 303(5–6) (1999), 467–474.
25. Z. Shi, Y. Lian, F.H. Liao, X. Zhou, Z. Gu, Y. Zhang, S. Iijima; "Large scale synthesis of single-wall carbon nanotubes by arc-discharge method", *J. Phys. Chem. Solids* 61(7) (2000), 1031–1036.
26. Y. Saito, K. Nishikubo, K. Kawabata, T. Matsumoto; "Carbon nanocapsules and single-layered nanotubes produced with platinum-group metals (Ru, Rh, Pd, Os, Ir, Pt) by arc discharge", *J. Appl. Phys.* 80(5) (1996), 3062–3067.
27. C. Liu, H.-M. Cheng, H.T. Cong, F. Li, G. Su, B.L. Zhou, M.S. Dresselhaus; "Synthesis of macroscopically long ropes of well-aligned single-wall carbon nanotubes", *Adv. Mater.* 12(16) (2000), 1190–1192.

28. T. Guo, P. Nikolaev, A. Thess, D.T. Colbert, R.E. Smalley; "Catalytic growth of single-walled nanotubes by laser vaporization", *Chem. Phys. Lett.* 243(1–2) (1995), 49–54.
29. A. Oberlin, M. Endo, T. Koyama; "High resolution electron microscope observations of graphitized carbon fibers", *J. Cryst. Growth* 14 (1976), 133–135.
30. N. Krishnakutty, N.M. Rodriguez, R.T.K. Baker; "Effect of copper on the decomposition of ethylene over an iron catalyst", *J. Catal.* 158(1) (1996), 217–227.
31. F.W.J. Van Hattum, J.M. Benito-Romero, A. Madronero, C.A. Bernado; "Morphological, mechanical and interfacial analysis of vapour-grown carbon fibres", *Carbon* 35(8) (1997), 1175–1183.
32. N.M. Rodriguez; "A review of catalytically grown carbon nanofibres", *J. Mater. Res.* 8(12) (1993), 3233–3250.
33. A.M. Benito, Y. Maniette, E. Munoz, M.T. Martinez; "Carbon nanotubes production by catalytic pyrolysis of benzene", *Carbon* 36(5) (1998), 681–683.
34. V. Ivanov, J.B. Nagy, P. Lambin, A. Lucas, X.B. Zhang, X.F. Zhang, D. Bernaerts, G. van Tendeloo, S. Amelinckx, J. van Landuyt; "The study of carbon nanotubules produced by catalytic method", *Chem. Phys. Lett.* 223(4) (1994), 329–335.
35. G.G. Tibbetts, D.W. Gorkiewicz, R.L. Alig; "A new reactor for growing carbon-fibers from liquid-phase and vapor-phase hydrocarbons", *Carbon* 31(5) (1993), 809–814.
36. W.Z. Li, S.S. Xie, L.X. Qian, B.H. Chang, B.S. Zou, W.Y. Zhou, R.A. Zhao, G. Wang; "Large-scale synthesis of aligned carbon nanotubes", *Science* 274(5293) (1996), 1701–1703.
37. M. Terrones, N. Grobert, J. Olivares, J.P. Zhang, H. Terrones, K. Kordatos, W.K. Hsu, J.P. Hare, P.D. Townsend, K. Prassides, A.K. Cheetham, H.W. Kroto, D.R.M. Walton; "Controlled production of aligned-nanotube bundles", *Nature* 388(6637) (1997), 52–55.
38. Z.F. Ren, Z.P. Huang, J.W. Xu, J.H. Wang, P. Bush, M.P. Siegel, P.N. Provenico; "Synthesis of large arrays of well-aligned carbon nanotubes on glass", *Science* 282(5391) (1998), 1105–1107.
39. C. Singh, M.S.P. Shaffer, I.A. Kinloch, A.H. Windle; "Production of aligned carbon nanotubes by the CVD injection method", *Physica B* 323(1–4) (2002), 339–340.
40. Z.W. Pan, S.S. Xie, B.H. Chang, C.Y. Wang, L. Lu, W. Liu, W.Y. Zhou, W.Z. Li, L.X. Qian; "Very long carbon nanotubes", *Nature* 394(6694) (1998), 631–632.
41. Z.P. Huang, J.W. Xu, Z.F. Ren, J.H. Wang, M.P. Siegel, P.N. Provenico; "Growth of highly oriented carbon nanotubes by plasma-enhanced hot filament chemical vapour deposition", *Appl. Phys. Lett.* 73(26) (1998), 3845–3847.
42. C. Bower, W. Zhu, D.J. Werder, O. Zhou; "Plasma-induced alignment of carbon nanotubes", *Appl. Phys. Lett.* 77(6) (2000), 830–832.
43. S. Hofmann, C. Ducati, J. Robertson, B. Kleinsorge; "Low-temperature growth of carbon nanotubes by plasma-enhanced chemical vapour deposition", *Appl. Phys. Lett.* 83(1) (2003), 135–137.

44. P. Nikolaev, M.J. Bronikowski, R.K. Bradley, F. Rohmund, D.T. Colbert, K.A. Smith, R.E. Smalley; "Gas-phase catalytic growth of single-walled carbon nanotubes from carbon monoxide", *Chem. Phys. Lett.* 313(1–2) (1999), 91–97.
45. S. Govindjee, J.L. Sackman; "On the use of continuum mechanics to estimate the properties of nanotubes", *Solid State Commun.* 110(4) (1999), 227–230.
46. M.M.J. Treacy, T.W. Ebbesen, J.M. Gibson; "Exceptionally high Young's modulus observed for individual carbon nanotubes", *Nature* 381(6584) (1996), 678–680.
47. A. Krishnan, E. Dujardin, T.W. Ebbesen, P.N. Yianilos, M.M.J. Treacy; "Young's modulus of single-walled nanotubes", *Phys. Rev. B* 58(20) (1998), 14013–14019.
48. P. Poncharal, Z.L. Wang, D. Ugarte, W.A. de Heer; "Electrostatic deflections and electromechanical resonances of carbon nanotubes", *Science* 283(5407) (1999), 1513–1516.
49. J.Z. Liu, Q. Zheng, Q. Jiang; "Effect of a rippling mode on resonances of carbon nanotubes", *Phys. Rev. Lett.* 86(21) (2001), 4843–4846.
50. M.R. Falvo, G.J. Clary, R.M. Taylor, V. Chi, F.P. Brooks Jr., S. Washburn, R. Superfine; "Bending and buckling of carbon nanotubes under large strain", *Nature* 389(6651) (1997), 582–584.
51. J.F. Despres, E. Daguerre, K. Lafdi; "Flexibility of graphene layers in carbon nanotubes", *Carbon* 33(1) (1995), 87–92.
52. R.S. Ruoff, D.C. Lorents; "Mechanical and thermal properties of carbon nanotubes", *Carbon* 33(7) (1995), 925–930.
53. S. Iijima, C. Brabec, A. Maiti, J. Bernholc; "Structural flexibility of carbon nanotubes", *J. Chem. Phys.* 104(5) (1996), 2089–2092.
54. O. Lourie, D.M. Cox, H.D. Wagner; "Buckling and collapse of embedded carbon nanotubes", *Phys. Rev. Lett.* 81(8) (1998), 1638–1641.
55. E.W. Wong, P.E. Shehan, C.M. Lieber; "Nanobeam mechanics: Elasticity, strength and toughness of nanorods and nanotubes", *Science* 277(5334) (1997), 1971–1975.
56. J.-P. Salvetat, A.J. Kulik, J.-M. Bonard, G.A.D. Briggs, T. Stöckli, K. Metenier, S. Bonnamy, F. Beguin, N.A. Burnham, L. Forro; "Elastic modulus of ordered and disordered multiwalled carbon nanotubes", *Adv. Mater.* 11(2) (1999), 161–165.
57. M.-F. Yu, O. Lourie, M.J. Dyer, K. Moloni, T.F. Kelly, R.S. Ruoff; "Strength and breaking mechanism of multiwalled carbon nanotubes under tensile load", *Science* 287(5453) (2000), 637–640.
58. M.-F. Yu, B.S. Files, A. Arepalli, R.S. Ruoff; "Tensile loading of ropes of single wall carbon nanotubes and their mechanical properties", *Phys. Rev. Lett.* 84(24) (2000), 5552–5555.
59. M.B. Nardelli, B.I. Yakobson, J. Bernholc; "Brittle and ductile behavior in carbon nanotubes", *Phys. Rev. Lett.* 81(21) (1998), 4656–4659.
60. J.P. Lu; "Elastic properties of carbon nanotubes and nanoropes", *Phys. Rev. Lett.* 79(7) (1997), 1297–1300.
61. N. Yao, V. Lordi; "Young's modulus of single-walled carbon nanotubes", *J. Appl. Phys.* 84(4) (1998), 1939–1943.
62. B.I. Yakobson, C.J. Brabec, J. Bernholc; "Nanomechanics of carbon tubes: Instabilities beyond linear response", *Phys. Rev. Lett.* 76(14) (1996), 2511–2514.

63. B.I. Yakobson, R.E. Smalley; "Fullerene nanotubes: $C_{1,000,000}$ and beyond", *Am. Sci.* 85(6) (1997), 324–337.
64. J. Bernholc, C.J. Brabec, M.B. Nardelli, A. Maiti, C. Roland, B.I. Yakobson; "Theory of growth and mechanical properties of nanotubes", *Appl. Phys. A* 67(1) (1998), 39–46.
65. T. Belytschko, S.P. Xiao, G.C. Schatz, R.S. Ruoff; "Atomistic simulation of nanotube fracture", *Phys. Rev. B* 65(235430) (2002).
66. D.A. Walters, L.M. Ericson, M.J. Casavant, J. Liu, D.T. Colbert, K.A. Smith, R.E. Smalley; "Elastic strain of freely suspended single-wall carbon nanotube ropes", *Appl. Phys. Lett.* 74(25) (1999), 3803–3805.
67. Z.W. Pan, S.S. Xie, L. Lu, B.H. Chang, L.F. Sun, W.Y. Zhou, G. Wang, D.L. Zhang; "Tensile tests of ropes of very long aligned multiwall carbon nanotubes", *Appl. Phys. Lett.* 74(21) (1999), 3152–3154.
68. H.D. Wagner, O. Lourie, Y. Feldmann, R. Tenne; "Stress-induced fragmentation of multiwall carbon nanotubes in a polymer matrix", *Appl. Phys. Lett.* 72(2) (1998), 188–190.
69. F. Li, H.M. Chai, S. Bai, G. Su, M.S. Dresselhaus; "Tensile strength of single-walled carbon nanotubes directly measured from their macroscopic ropes", *Appl. Phys. Lett.* 77(20) (2000), 3161–3163.
70. L.S. Schadler, S.C. Giannaris, P.M. Ajayan; "Load transfer in carbon nanotubes epoxy composites", *Appl. Phys. Lett.* 73(26) (1998), 3842–3844.
71. C.L. Kane, E.J. Mele; "Size, shape, and low energy electronic structure of carbon nanotubes", *Phys. Rev. Lett.* 78(10) (1997), 1932–1935.
72. R. Saito, M. Fujita, G. Dresselhaus, M.S. Dresselhaus; "Electronic structure of chiral graphene tubules", *Appl. Phys. Lett.* 60(18) (1992), 2204–2206.
73. N. Hamada, S.-I. Sawada, A. Oshiyama; "New one-dimensional conductors: Graphitic microtubules", *Phys. Rev. Lett.* 68(10) (1992), 1579–1581.
74. J.W. Mintmire, B.I. Dunlop, C.T. White; "Are fullerene tubules metallic?", *Phys. Rev. Lett.* 68(5) (1992), 631–634.
75. C.T. White, D.H. Robertson, J.W. Mintmire; "Helical and rotational symmetries of nanoscale graphitic tubules", *Phys. Rev. B* 47(9) (1993), 5485–5488.
76. J.W. Mintmire, C.T. White; "Electronic and structural properties of carbon nanotubes", *Carbon* 33(7) (1995), 893–902.
77. L.X. Benedict, V.H. Crespi, S.G. Louie, M.L. Cohen; "Static conductivity and superconductivity of carbon nanotubes: Relations between tubes and sheets", *Phys. Rev. B* 52(20) (1995), 14935–14940.
78. K. Tanaka, H. Aoki, H. Ago, T. Yamabe, K. Okahara; "Interlayer interaction of two graphene sheets as a model of double-layer carbon nanotubes", *Carbon* 35(1) (1997), 121–125.
79. P. Lambin, V. Meunier, A. Rubio; "Electronic structure of polychiral carbon nanotubes", *Phys. Rev. B* 62(8) (2000), 5129–5135.
80. L. Langer, L. Stockman, J.P. Heremans, V. Bayot, C.H. Olk, C. van Haesendonck, Y. Bruynseraede, J.P. Issi; "Electrical resistance of a carbon nanotube bundle", *J. Mater. Res.* 9(4) (1994), 927–932.

81. J.P. Heremans, C.H. Olk, D.T. Morelli; "Magnetic susceptibility of carbon structures", *Phys. Rev. B* 49(21) (1994), 15122–15125.
82. T.W. Ebbesen, H.J. Lezec, H. Hiura, J.W. Bennett, H.F. Ghaemie, T. Thio; "Electrical conductivity of individual carbon nanotubes", *Nature* 382(6586) (1996), 54–56.
83. S.J. Tans, M.H. Devoret, H. Dai, A. Thess, R.E. Smalley, L.J. Geerligs, C. Dekker; "Individual single-wall carbon nanotubes as quantum wires", *Nature* 386(6624) (1997), 474–477.
84. T.W. Odom, J.-L. Huang, P. Kim, C.M. Lieber; "Atomic structure and electronic properties of single-walled carbon nanotubes", *Nature* 391(6662) (1998), 62–64.
85. J.W.G. Wildöer, L.C. Venema, A.G. Rinzler, R.E. Smalley, C. Dekker; "Electronic structure of atomically resolved carbon nanotubes", *Nature* 391(6662) (1998), 59–62.
86. M. Bockrath, D.H. Cobden, P.L. McEuen, N.G. Chopra, A. Zettl, A. Thess, R.E. Smalley; "Single-electron transport in ropes of carbon nanotubes", *Science* 275(5308) (1997), 1922–1925.
87. G.T. Kim, E.S. Choi, D.C. Kim, D.S. Suh, Y.W. Park, K. Liu, G. Duesberg, S. Roth; "Magnetoresistance of an entangled single-wall carbon-nanotube network", *Phys. Rev. B* 58(24) (1998), 16064–16069.
88. J.E. Fischer, H. Dai, A. Thess, R. Lee, N.M. Hanjani, D.L. Dehaas, R.E. Smalley; "Metallic resistivity in crystalline ropes of single-wall carbon nanotubes", *Phys. Rev. B* 55(8) (1997), 4921–4924.
89. A.D. Bozhko, D.E. Sklovsky, V.A. Nalimova, A.G. Rinzler, R.E. Smalley, J.E. Fischer; "Resistance vs. pressure of single-wall carbon nanotubes", *Appl. Phys. A* 67(1) (1998), 75–77.
90. J.R. Charlier, J.-P. Issi; "Electrical conductivity of novel forms of carbon", *J. Phys. Chem. Solids* 57(6–8) (1996), 957–965.
91. J.-O. Lee, C. Park, J.-J. Kim, J. Kim, J.W. Park, K.-H. Yoo; "Formation of low-resistance ohmic contact between carbon nanotubes and metal electrodes by a rapid thermal annealing method", *J. Phys. D: Appl. Phys.* 33(16) (2000), 1953–1956.
92. H. Dai, E.W. Wong, C.M. Lieber; "Probing electrical transport in nanomaterials: Conductivity of individual carbon nanotubes", *Science* 272(5261) (1996), 523–526.
93. A.B. Kaiser, G.S. Duesberg, S. Roth; "Heterogeneous model for conduction in carbon nanotubes", *Phys. Rev. B* 57(3) (1998), 1418–1421.
94. J. Hone, M. Whitney, A. Zettl; "Thermal conductivity of single-walled carbon nanotubes", *Synth. Metals* 103(1–3) (1999), 2498–2499.
95. P. Kim, L. Shi, A. Majumdar, P.L. McEuen; "Thermal transport measurements of individual multiwalled nanotubes", *Phys. Rev. Lett.* 87(215502) (2001).
96. P.M. Ajayan, O. Stephan, C. Colliex, D. Trauth; "Aligned carbon nanotube arrays formed by cutting a polymer resin-nanotube composite", *Science* 265(5176) (1994), 1212–1214.
97. L.A. Bursill, J.L. Peng, X.D. Fan; "Cross-sectional high-resolution transmission electron-microscopy study of the structures of carbon nanotubes", *Phil. Mag.* A 71(5) (1995), 1161–1176.

98. O. Lourie, H.D. Wagner; "Transmission electron microscopy observations of fracture of single-wall carbon nanotubes under axial tension", *Appl. Phys. Lett.* 73(24) (1998), 3527–3529.
99. O. Lourie, H.D. Wagner; "Evidence of stress transfer and formation of fracture clusters in carbon nanotube-based composites", *Comp. Sci. Tech.* 59(6) (1999), 975–977.
100. P.M. Ajayan, L.S. Schadler, C. Giannaris, A. Rubio; "Single-walled carbon nanotube-polymer composites: strength and weaknesses", *Adv. Mater.* 12(10) (2000) 750–752
101. M.S.P. Shaffer, X. Fan, A.H. Windle; "Dispersion and packing of carbon nanotubes", *Carbon* 36(11) (1998), 1603–1612.
102. K.T. Lau, S.-Q. Shi, H.-M. Cheng; "Micro-mechanical properties and morphological observation on fracture surfaces of carbon nanotube composites pre-treated at different temperatures", *Comp. Sci. Tech.* 63(8) (2003), 1161–1164.
103. J.B. Bai, A. Allaoui; "Effect of the length and the aggregate size of MWCNTs on the improvement efficiency of the mechanical and electrical properties of nanocomposites – experimental investigation", *Comp. Part A* 34(8) (2003), 689–694.
104. X. Gong, J. Liu, S. Baskaran, R.D. Voise, J.S. Young; "Surfactant-assisted processing of carbon nanotube/polymer composites", *Chem. Mater.* 12(4) (2000), 1049–1052.
105. J. Zhu, J.D. Kim, H. Peng, J.L. Margrave, V.N. Khabashesku, E.V. Barrera; "Improving the dispersion and integration of single-wall carbon nanotubes in epoxy composites through functionalisation", *Nano Lett.* 3(8) (2003), 1107–1113.
106. M.S.P. Shaffer, A.H. Windle; "Fabrication and characterization of carbon nanotube/poly(vinyl alcohol) composites", *Adv. Mater.* 11(11) (1999), 937–941.
107. M.S.P. Shaffer; "Carbon nanotubes", PhD thesis, University of Cambridge, UK (1998).
108. J. Liu, A.G. Rinzler, H.J. Dai, J.H. Hafner, R.K. Bradley, P.J. Boul, A. Lu, T. Iverson, K. Shelimov, C.B. Huffman, F. Rodriguez-Macias, Y.S. Shon, T.R. Lee, D.T. Colbert, R.E. Smalley; "Fullerene pipes", *Science* 280(5367) (1998), 1253–1256.
109. N. Yao, V. Lordi, S.X.C. Ma, E. Dujardin, A. Krishnan, M.M.J. Treacy, T.W. Ebbesen; "Structure and oxidation patterns of carbon nanotubes", *J. Mater. Res.* 13(9) (1998), 2432–2437.
110. E.T. Mickelson, I.W. Chiang, J.L. Zimmermann, P.J. Boul, J. Lozano, J. Liu, R.E. Smalley, R.H. Hauge, J.L. Margrave; "Solvation of fluorinated single-wall carbon nanotubes in alcohol solvents", *J. Phys. Chem. B* 103(21) (1999), 4318–4322.
111. F.H. Gojny, J. Nastalczyk, Z. Roslaniec, K. Schulte; "Surface modified multi-wall carbon nanotubes in CNT/epoxy-composites", *Chem. Phys. Lett.* 370(5–6) (2003), 820–824.
112. R.D. Patton, C.U. Pittman Jr., L. Wang J.R. Hill; "Vapor grown carbon fiber composites with epoxy and poly(phenylene sulfide) matrices", *Comp. Part A* 30(9) (1999), 1081–1091.

113. R.D. Patton, C.U. Pittman Jr., L. Wang, J.R. Hill, A. Day; "Ablation, mechanical and thermal conductivity of vapor grown carbon fiber/phenolic matrix composites", *Comp. Part A* 33(2) (2002), 243–251.
114. D. Puglia, L. Valentini, J.M. Kenny; "Analysis of the cure reaction of carbon nanotubes/epoxy resin composites through thermal analysis and Raman spectroscopy", *J. Appl. Polym. Sci.* 88(2) (2003), 452–458.
115. M. Yin, J.A. Koutsky, T.L. Barr, N.M. Rodriguez, R.T.K. Baker, L. Klebanov; "Characterization of carbon microfibers as a reinforcement for epoxy resins", *Chem. Mater.* 5(7) (1993), 1024–1031.
116. J. Sandler, M.S.P. Shaffer, T. Prasse, W. Bauhofer, K. Schulte, A.H. Windle; "Development of a dispersion process for carbon nanotubes in an epoxy matrix and the resulting electrical properties", *Polymer* 40(21) (1999), 5967–5971.
117. A. Allaoui, S. Bai, H.M. Cheng, J.B. Bai; "Mechanical and electrical properties of a MWNT/epoxy composite", *Comp. Sci. Tech.* 62(15) (2002), 1993–1998.
118. S. Barrau, P. Demont, A. Peigny, C. Laurent, C. Lacabanne; "DC and AC conductivity of carbon nanotubes-polyepoxy composites", *Macromolecules* 36(14) (2003), 5187–5194.
119. T. Prasse, J.-Y. Cavaille, W. Bauhofer; "Electric anisotropy of carbon nanofibre/epoxy resin composites due to electric field induced alignment", *Comp. Sci. Tech.* 63(13) (2003), 1835–1841.
120. L. Valentini, D. Puglia, E. Frulloni, I. Armentano, J.M. Kenny, S. Santucci; "Dielectric behavior of epoxy matrix/single-walled carbon nanotube composites", *Comp. Sci. Tech.* 64(1) (2004), 23–33.
121. J.K.W. Sandler, J.E. Kirk, I.A. Kinloch, M.S.P. Shaffer, A.H. Windle; "Ultra-low electrical percolation threshold in carbon-nanotube-epoxy composites", *Polymer* 44(19) (2003), 5893–5899.
122. C.A. Martin, J.K.W. Sandler, M.S.P. Shaffer, M.-K. Schwarz, W. Bauhofer, K. Schulte, A.H. Windle; "Formation of percolating networks in multi-wall carbon-nanotube-epoxy composites", *Comp. Sci. Tech.* 64(15) (2004), 2309–2316.
123. C.A. Martin, J.K.W. Sandler, A.H. Windle, M.-K. Schwarz, W. Bauhofer, K. Schulte, M.S.P. Shaffer; "Electric field-induced aligned multi-wall carbon nanotube networks in epoxy composites", *Polymer* 46(3) (2005), 877–886.
124. M.J. Biercuk, M.C. Llaguno, M. Radosavljevic, J.K. Hyun, A.T. Johnson, J.E. Fischer; "Carbon nanotube composites for thermal management", *Appl. Phys. Lett.* 80(15) (2002), 2767–2769.
125. R.L. Vander Wal, L.J. Hall; "Nanotube coated metals: New reinforcement materials for polymer matrix composites", *Adv. Mater.* 14(18) (2002), 1304–1308.
126. E.T. Thostenson, W.Z. Li, D.Z. Wang, Z.F. Ren, T.-W. Chou; "Carbon nanotube/carbon fiber hybrid multiscale composites", *J. Appl. Phys.* 91(9) (2002), 6034–6037.
127. W.B. Downs, R.T.K. Baker; "Modification of the surface properties of carbon fibers via the catalytic growth of carbon nanofibres", *J. Mater. Res.* 10(3) (1995), 625–633.
128. M.D. Frogley, D. Ravich, H.D. Wagner; "Mechanical properties of carbon nanoparticle-reinforced elastomers", *Comp. Sci. Tech.* 63(11) (2003), 1647–1654.

129. P. Richard, T. Prasse, J-Y. Cavaille, L. Chazeau, C. Gauthier, J. Duchet; "Reinforcement of rubbery epoxy by carbon nanofibres", *Mater. Sci. Eng. A* 352(1-2) (2003), 344-348.
130. M.A. Osman, A. Atallah, M. Müller, U.W. Sluter; "Reinforcement of poly(dimethylsiloxane) networks by mica flakes", *Polymer* 42(15) (2001), 6545-6556.
131. J.B. Donnet; "Nano and microcomposites of polymers, elastomers and their reinforcement", *Comp. Sci. Tech.* 63(8) (2003), 1085-1088.
132. G. Heinrich, M. Klüppel, T.A. Vilgis; "Reinforcement of elastomers", *Curr. Opin. Solid State Mater. Sci.* 6(3) (2002), 195-203.
133. C.A. Cooper, D. Ravich, D. Lips, J. Mayer, H.D. Wagner; "Distribution and alignment of carbon nanotubes and nanofibrils in a polymer matrix", *Comp. Sci. Tech.* 62(7-8) (2002), 1105-1112.
134. W. Tang, M.H. Santare, S.G. Advani; "Melt processing and mechanical property characterization of multi-walled carbon nanotube/high density polyethylene (MWNT/HDPE) composite films", *Carbon* 41(14) (2003), 2779-2785.
135. E.T. Thostenson, T.-W. Chou; "Aligned multi-walled carbon nanotube-reinforced composites: processing and mechanical characterization", *J. Phys. D: Appl. Phys.* 35(16) (2002), 77-80.
136. Z. Jin, K.P. Pramoda, S.H. Goh, G. Xu; "Poly(vinylidene fluoride)-assisted melt-blending of multi-walled carbon nanotube/poly(methyl methacrylate) composites", *Mater. Res. Bull.* 37(2) (2002), 271-278.
137. K. Lozano, E.V. Barrera; "Nanofiber-reinforced thermoplastic composites I: Thermoanalytical and mechanical analyses", *J. Appl. Polym. Sci.* 79(1) (2001), 125-133.
138. Z. Jin, K.P. Pramoda, G. Xu, S.H. Goh; "Dynamic mechanical behavior of melt-processed multi-walled carbon nanotube/poly(methyl methacrylate) composites", *Chem. Phys. Lett.* 337(1-3) (2001), 43-47.
139. P. Pötschke, T.D. Fornes, D.R. Paul; "Rheological behavior of multiwalled carbon nanotube/polycarbonate composites", *Polymer* 43(11) (2002) 3247-3255.
140. P. Pötschke, S.M. Dudkin, I. Alig; "Dielectric spectroscopy on melt processed polycarbonate-multiwalled carbon nanotube composites", *Polymer* 44(17) (2003), 5023-5030.
141. O. Meincke, D. Kaempfer, H. Weickmann, C. Friedrich, M. Vathauer, H. Warth; "Mechanical properties and electrical conductivity of carbon-nanotube filled polyamide-6 and its blends with acrylonitrile/butadiene/styrene" *Polymer* 45(3) (2004), 739-748.
142. J.K.W. Sandler, S. Pegel, M. Cadek, F. Gojny, M. van Es, J. Lohmar, W.J. Blau, K. Schulte, A.H. Windle, M.S.P. Shaffer; "A comparative study of melt-spun polyamide-12 fibres reinforced with carbon nanotubes and nanofibres", *Polymer* 45(6) (2004), 2001-2015.
- 143 G.G. Tibbetts, J.J. McHugh; "Mechanical properties of vapor-grown carbon fiber composites with thermoplastic matrices", *J. Mater. Res.* 14(7) (1999), 2871-2880.

144. R.J. Kuriger, M.K. Alam, D.P. Anderson, R.L. Jacobsen; "Processing and characterization of aligned vapor grown carbon fiber reinforced polypropylene", *Comp. Part A* 33(1) (2002), 53–62.
145. K. Lozano, J. Bonilla-Rios, E.V. Barrera; "A study on nanofiber-reinforced thermoplastic composites II: Investigation of the mixing rheology and conduction properties", *J. Appl. Polym. Sci.* 80(8) (2001), 1162–1172.
146. O.S. Carneiro, J.A. Covas, C.A. Bernado, G. Caldeira, F.W.J. Van Hattum, J.-M. Ting, R.L. Alig, M.L. Lake; "Production and assessment of polycarbonate composites reinforced with vapour-grown carbon fibres", *Comp. Sci. Tech.* 58(3–4) (1998), 401–407.
147. A. Ramazani, A. Ait-Kadi, M. Grmela; "Rheological modelling of short fiber thermoplastic composites", *J. Non-Newton. Fluid Mech.* 73(3) (1997), 241–260.
148. P. Cortes, K. Lozano, E.V. Barrera, J. Bonilla-Rios; "Effects of nanofiber treatments on the properties of vapor-grown carbon fiber reinforced polymer composites", *J. Appl. Polym. Sci.* 89(9) (2003), 2527–2534.
149. D. Qian, E.C. Dickey, R. Andrews, T. Rantell; "Load transfer and deformation mechanisms in carbon nanotube-polystyrene composites", *Appl. Phys. Lett.* 76(20) (2000), 2868–2870.
150. P.C. Watts, W.K. Hsu, G.Z. Chen, D.J. Fray, H.W. Kroto, D.R.M. Walton; "A low resistance boron-doped carbon nanotube-polystyrene composite", *J. Mater. Chem.* 11(10) (2001), 2482–2488.
151. B. Safadi, R. Andrews, E.A. Grulke; "Multiwalled carbon nanotube polymer composites: synthesis and characterization of thin films", *J. Appl. Polym. Sci.* 84(14) (2002), 2660–2669.
152. L. Jin, C. Bower, O. Zhou; "Alignment of carbon nanotubes in a polymer matrix by mechanical stretching", *Appl. Phys. Lett.* 73(9) (1998), 1197–1199.
153. C. Bower, R. Rosen, J. Han, O. Zhou; "Deformation of carbon nanotubes in nanotube-polymer composites", *Appl. Phys. Lett.* 74(22) (1999), 3317–3319.
154. M. Cadek, J.N. Coleman, V. Barron, K. Hedicke, W.J. Blau; "Morphological and mechanical properties of carbon-nanotube-reinforced semicrystalline and amorphous polymer composites", *Appl. Phys. Lett.* 81(27) (2002), 5123–5125.
155. S.L. Ruan, P. Gao, X.G. Yang, T.X. Yu; "Toughening high performance ultrahigh molecular weight polyethylene using multiwalled carbon nanotubes", *Polymer* 44(19) (2003), 5643–5654.
156. E. Assouline, A. Lustiger, A.H. Barber, C.A. Cooper, E. Klein, E. Wachtel, H.D. Wagner; "Nucleation ability of multiwall carbon nanotubes in polypropylene composites", *J. Polym. Sci. B: Polym. Phys.* 41(5) (2003), 520–527.
157. B.P. Grady, F. Pompeo, R.L. Shambaugh, D.E. Resasco; "Nucleation of polypropylene crystallization by single-walled carbon nanotubes", *J. Phys. Chem. B* 106(23) (2002), 5852–5858.
158. M.C. Paiva, B. Zhou, K.A.S. Fernando, Y. Lin, J.M. Kennedy, Y.-P. Sun; "Mechanical and morphological characterization of polymer-carbon nanocomposites from functionalized carbon nanotubes", *Carbon* 42(14) (2004), 2849–2854.

159. O. Probst, E.M. Moore, D.E. Resasco, B.P. Grady; "Nucleation of polyvinyl alcohol crystallization by single-walled carbon nanotubes", *Polymer* 45(13) (2004), 4437–4443.
160. X. Zhang, T. Liu, T.V. Sreekumar, S. Kumar, V.C. Moore, R.H. Hauge, R.E. Smalley; "Poly(vinyl alcohol)/SWCNT composite film", *Nano Lett.* 3(9) (2003), 1285–1288.
161. K.L. Lu, R.M. Lago, Y.K. Chen, M.L.H. Green, P.F. Harris, S.C. Tsang; "Mechanical damage of carbon nanotubes by ultrasound", *Carbon* 34(6) (1996), 814–816.
162. A. Koshio, M. Yudasaka, M. Zhang, S. Iijima; "A simple way to chemically react single-wall carbon nanotubes with organic materials using ultrasonication", *Nano Lett.* 1(7) (2001), 361–363.
163. A. Dufresne, M. Paillet, J.L. Putaux, R. Canet, F. Carmona, P. Delhaes, S. Cui; "Processing and characterization of carbon nanotube/poly(styrene-co-butyl acrylate) nanocomposites", *J. Mater. Sci.* 37(18) (2002), 3915–3923.
164. Y. Lin, B. Zhou, K.A.S. Fernando, P. Liu, L.A. Allard, Y.-P. Sun; "Polymeric carbon nanocomposites from carbon nanotubes functionalised with matrix polymer", *Macromolecules* 36(19) (2003), 7199–7204.
165. C.A. Mitchell, J.L. Bahr, S. Arepalli, J.M. Tour, R. Krishnamoorti; "Dispersion of functionalized carbon nanotubes in polystyrene", *Macromolecules* 35(23) (2002), 8825–8830.
166. Z.J. Jia, Z.Y. Wang, C.L. Xu, J. Liang, B.Q. Wei, D.H. Wu, S.W. Zhu; "Study on poly(methyl methacrylate)/carbon nanotube composites", *Mater. Sci. Eng. A* 271(1–2) (1999), 395–400.
167. S. Kumar, T.D. Dang, F.E. Arnold, A.R. Bhattacharyya, B.G. Min, X. Zhang, R.A. Vaia, C. Park, W.W. Adams, R.H. Hauge, R.E. Smalley, S. Ramesh, P.A. Willis; "Synthesis, structure, and properties of PBO/SWNT composites", *Macromolecules* 35(24) (2002), 9039–9043.
168. H.J. Barraza, F. Pompeo, E.A. O'Rear, D.E. Resasco; "SWNT-filled thermoplastic and elastomeric composites prepared by miniemulsion polymerization", *Nano Lett.* 2(8) (2002), 797–802.
169. Z. Ounaies, C. Park, K.E. Wise, E.J. Siochi, J.S. Harrison; "Electrical properties of single wall carbon nanotube reinforced polyimide composites", *Comp. Sci. Tech.* 63(11) (2003), 1637–1646.
170. Z. Roslaniec, G. Broza, K. Schulte; "Nanocomposites based on multiblock polyester elastomers (PEE) and carbon nanotubes (CNT)", *Comp. Interfaces* 10(1) (2003), 95–102.
171. M.J. O'Connell, P. Boul, L.M. Ericson, C. Huffman, Y. Wang, E. Haroz, C. Kuper, J. Tour, K.D. Ausman, R.E. Smalley; "Reversible water-solubilization of single-walled carbon nanotubes by polymer wrapping", *Chem. Phys. Lett.* 342(3–4) (2001), 265–271.
172. J. Sandler, P. Werner, M.S.P. Shaffer, V. Demchuk, V. Altstädt, A.H. Windle; "Carbon-nanofibre-reinforced poly(ether ether ketone) composites", *Comp. Part A* 33(8) (2002), 1033–1039.

173. T. Kimura, H. Ago, M. Tobita, S. Ohshima, M. Kyotani, M. Yumura; "Polymer composites of carbon nanotubes aligned by a magnetic field", *Adv. Mater.* 14(19) (2003), 1380–1383.
174. R. Andrews, D. Jacques, A.M. Rao, T. Rantell, F. Derbyshire, Y. Chen, J. Chen, R.C. Haddon; "Nanotube composite carbon fibers", *Appl. Phys. Lett.* 75(9) (1999), 1329–1331.
175. S.A. Gordeyev, J.A. Ferreira, C.A. Bernado, I.M. Ward; "A promising conductive material: highly oriented polypropylene filled with short vapour-grown carbon fibres", *Mater. Lett.* 51(1) (2001), 32–36.
176. S. Kumar, H. Doshi, M. Srinivasarao, J.O. Park, D.A. Schiraldi; "Fibers from polypropylene/nano carbon fiber composites", *Polymer* 43(5) (2002), 1701–1703.
177. J.C. Kearns, R.L. Shambaugh; "Polypropylene fibers reinforced with carbon nanotubes", *J. Appl. Polym. Sci.* 86(8) (2002), 2079–2084.
178. H. Ma, J. Zeng, M.L. Realff, S. Kumar, D.A. Schiraldi; "Processing, structure, and properties of fibers from polyester/carbon nanofiber composites", *Comp. Sci. Tech.* 63(11) (2003), 1617–1628.
179. A.R. Bhattacharyya, T.V. Sreekumar, T. Liu, S. Kumar, L.M. Ericson, R.H. Hauge, R.E. Smalley; "Crystallization and orientation studies in polypropylene/single wall carbon nanotube composites", *Polymer* 44(8) (2003), 2373–2377.
180. J. Zeng, B. Saltysiak, W.S. Johnson, D.A. Schiraldi, S. Kumar; "Processing and properties of poly(methyl methacrylate)/carbon nano fiber composites", *Comp. Part B* 35(2) (2004), 173–178.
181. J. Sandler, A.H. Windle, P. Werner, V. Altstädt, M. van Es, M.S.P. Shaffer; "Carbon-nanofibre-reinforced poly(ether ether ketone) fibres", *J. Mater. Sci.* 38(10) (2003), 2135–2141.
182. P. Werner, R. Verdejo, F. Wöllecke, V. Altstädt, J.K.W. Sandler, M.S.P. Shaffer; "Carbon nanofibers allow foaming of semicrystalline poly(ether ether ketone)", *Adv. Mater.* 17(23) (2005), 2864–2869.
183. N.S. Ramesh, S.T. Lee; "Blowing agent effect on extensional viscosity calculated from fiber spinning method for foam processing", *J. Cell. Plast.* 36(5) (2000), 374–385.
184. D.S. Bangarusampath, H. Ruckdäschel, J.K.W. Sandler, V. Altstädt, M.S.P. Shaffer; "Rheological properties of carbon nanofibre reinforced poly(ether ether ketone) composites under shear and elongational flow", *Polymer* (2006), submitted.
185. B. Vigolo, A. Penicaud, C. Coulon, C. Sauder, R. Pailler, C. Journet, P. Bernier, P. Poulin; "Macroscopic fibers and ribbons of oriented carbon nanotubes", *Science* 290(5495) (2000), 1331–1334.
186. A.B. Dalton, S. Collins, E. Munoz, J.M. Razal, V.H. Ebron, J.P. Ferraris, J.N. Coleman, B.G. Kim, R.H. Baughman; "Super-tough carbon-nanotube fibres – These extraordinary composite fibres can be woven into electronic textiles", *Nature* 423(6941) (2003), 703.
187. L.M. Ericson, H. Fan, H.Q. Peng, V.A. Davis, W. Zhou, J. Sulpizio, Y.H. Wang, R. Booker, J. Vavro, C. Guthy, A.N.G. Parra-Vasquez, M.J. Kim, S. Ramesh, R.K. Saini, C. Kittrell, G. Lavin, H. Schmidt, W.W. Adams, W.E. Billups, M. Pasquali,

- W.F. Hwang, R.H. Hauge, J.E. Fischer, R.E. Smalley; "Macroscopic, neat, single-walled carbon nanotube fibers", *Science* 305(5689) (2004), 1447–1450.
188. W. Zhou, J. Vavro, C. Guthy, K.I. Winey, J.E. Fischer, L.M. Ericson, S. Ramesh, R. Saini, V.A. Davis, C. Kittrell, M. Pasquali, R.H. Hauge, R.E. Smalley; "Single wall carbon nanotube fibers extruded from super-acid suspensions: Preferred orientation, electrical, and thermal transport", *J. Appl. Phys.* 95(2) (2004), 649–655.
189. A.A. Mamedov, N.A. Kotov, M. Prato, D.M. Guldi, J.P. Wicksted, A. Hirsch; "Molecular design of strong single-wall carbon nanotube/polyelectrolyte multilayer composites", *Nature Mat.* 1(3) (2002), 190–194.
190. S.S. Ray, M. Okamoto; "Polymer/layered silicate nanocomposites: a review from preparation to processing", *Prog. Polym. Sci.* 28(11) (2003), 1539–1641.
191. F.W.J. Van Hattum, C.A. Bernado, J.C. Finegan, G.G. Tibbetts, R.L. Alig, M.L. Lake; "A study of the thermomechanical properties of carbon fiber-reinforced polypropylene composites", *Polym. Comp.* 20(5) (1999), 683–688.
192. J.K.W. Sandler; "Structure-property-relationships of carbon nanotubes / nanofibres and their polymer composites", PhD thesis, University of Cambridge, UK (2005).
193. G. Tsagaropoulos, A. Eisenberg; "Dynamic mechanical study of the factors affecting the two glass transition behavior of filled polymers. Similarities and differences with random ionomers", *Macromolecules* 28(18) (1995), 6067–6077.
194. P. Werner, V. Altstadt, R. Jaskulka, O. Jacobs, J.K.W. Sandler, M.S.P. Shaffer, A.H. Windle; "Tribological behaviour of carbon-nanofibre-reinforced poly(ether ether ketone)", *Wear* 257(9–10) (2004), 1006–1014.
195. Y.S. Zoo, J.W. An, D.P. Lim, D.S. Lim; "Effect of carbon nanotube addition on tribological behavior of UHMWPE", *Tribol. Lett.* 16(4) (2004), 305–309.
196. M.J. Folkes, D.A.M. Russell; "Orientation effects during the flow of short-fibre reinforced thermoplastics", *Polymer* 21() (1980), 1252–1258.
197. S.E. Barbosa, D.R. Ercoli, M.A. Bibbo, J.M. Kenny; "Rheology of short-fiber composites: A systematic approach", *Comp. Struct.* 27(1–2) (1994), 83–91.
198. J. Sandler, G. Broza, M. Nolte, K. Schulte, Y.-M. Lam, M.S.P. Shaffer; "Crystallization of carbon nanotube and nanofiber polypropylene composites", *J. Macromol. Sci. B: Phys.* B42(3–4) (2003), 479–488.
199. L. Valentini, J. Biagiotti, J.M. Kenny, S. Santucci; "Morphological characterization of single-walled carbon nanotubes-PP composites", *Comp. Sci. Tech.* 63(8) (2003), 1149–1153.
200. M. Mucha, J. Marszalek, A. Fidrych; "Crystallization of isotactic polypropylene containing carbon black as a filler", *Polymer* 41(11) (2000), 4137–4142.
201. W. Xu, M. Ge, P. He; "Nonisothermal crystallization kinetics of polypropylene/montmorillonite nanocomposites", *J. Polym. Sci. B: Polym. Phys.* 40(5) (2002), 408–414.
202. N. Levi, R. Czerw, S.Y. Xing, P. Iyer, D.L. Carroll; "Properties of polyvinylidene difluoride-carbon nanotube blends", *Nano Lett.* 4(7) (2004), 1267–1271.
203. T. Kitao, S. Ohya, J. Furukawa, S. Yamashita; "Orientation of polymer molecules during melt spinning. II. Orientation of crystals in as-spun polyolefin fibers", *J. Polym. Sci. - Polym. Phys. Ed.* 11 (1973), 1091–1109.

204. F.M. Lu, J.E. Spruiell; "The role of crystallization kinetics in the development of the structure and properties of polypropylene filaments", *J. Appl. Polym. Sci.* 49(4) (1993), 623–631.
205. A. Marcincin; "Modification of fiber-forming polymers by additives", *Prog. Polym. Sci.* 27(5) (2002), 853–913.
206. Y.L. Li, I.A. Kinloch, A.H. Windle; "Direct spinning of carbon nanotube fibers from chemical vapor deposition synthesis", *Science* 304(5668) (2004), 276–27.
207. H.J. Mair, S. Roth, Eds.; "Elektrisch leitende Kunststoffe", Carl Hanser Hamburg, Germany, (1989).
208. R. Zallen; "The physics of amorphous solids", John Wiley & Sons, New York (1983).
209. D. Stauffer; "Introduction to percolation theory", Taylor & Francis, London (1984).
210. F. Lux; "Models proposed to explain the electrical conductivity of mixtures made of conductive and insulating materials", *J. Mater. Sci.* 28(2) (1993), 285–301.
211. F. Carmona, P. Prudhorn, F. Barreau; "Percolation in short fibers epoxy-resin composites – conductivity behaviour and finite size effects near threshold", *Solid State Commun.* 51(4) (1984), 255–257.
212. M.T. Connor, S. Roy, T.A. Ezquerra, F.J. Balta-Calleja; "Broadband AC conductivity of conductor-polymer composites", *Phys. Rev. B* 57(4) (1998), 2286–2294.
213. S.A. Gordeyev, F.J. Macedo, J.A. Ferreira, F.W.J. Van Hattum, C.A. Bernado; "Transport properties of polymer-vapour-grown carbon fibre composites", *Physica B* 279(1–3) (2000), 33–36.
214. I.C. Finegan, G.G. Tibbetts; "Electrical conductivity of vapor-grown carbon fiber/thermoplastic composites", *J. Mater. Res.* 16(6) (2001), 1668–1674.
215. B.E. Kilbride, J.N. Coleman, J. Fraysse, P. Fournet, M. Cadek, A. Drury, S. Hutzler, S. Roth, W.J. Blau; "Experimental observation of scaling laws for alternating and direct current conductivity in polymer-carbon nanotube composite thin films", *J. Appl. Phys.* 92(7) (2002), 4024–4030.
216. C. Stephan, T.P. Nguyen, B. Lahr, W.J. Blau, S. Lefrant, O. Chauvet; "Raman spectroscopy and conductivity measurements on polymer-multiwalled carbon nanotubes composites", *J. Mater. Res.* 17(2) (2002), 396–400.
217. P. Pötschke, A.R. Bhattacharyya, A. Janke; "Morphology and electrical resistivity of melt mixed blends of polyethylene and carbon nanotube filled polycarbonate", *Polymer* 44(26) (2003), 8061–8069.
218. M. Wu, L.L. Shaw; "On the improved properties of injection-molded, carbon nanotube-filled pet/pvdf blends", *J. Power Sources* 136(1) (2004), 37–44.
219. M. Sumita, K. Sakata, S. Asai, K. Miyasaka, H. Nakagawa; "Dispersion of fillers and the electrical-conductivity of polymer blends filled with carbon black", *Polym. Bull.* 25(2) (1991), 265–271.
220. C. Zhang, X.S. Yi, H. Yui, S. Asai, M. Sumita; "Morphology and electrical properties of short carbon fiber-filled polymer blends: High-density polyethylene poly(methyl methacrylate)", *J. Appl. Polym. Sci.* 69(9) (1998), 1813–1819.
221. S.-Y. Fu, Y.-W. Mai; "Thermal conductivity of misaligned short-fiber-reinforced polymer composites", *J. Appl. Polym. Sci.* 88(6) (2003), 1497–1505.

222. V. Jamieson; "Whatever happened to nanotubes, the hollow threads of carbon that were going to change the world?", *New Scientist* 2386, 15 March (2003).
223. F.T. Fisher, R.D. Bradshaw, L.C. Brinson; "Effects of nanotube waviness on the modulus of nanotube-reinforced polymers", *Appl. Phys. Lett.* 80(24) (2002), 4647–4649.
224. A.H. Barber, S.R. Cohen, H.D. Wagner; "Measurement of carbon nanotube-polymer interfacial strength", *Appl. Phys. Lett.* 82(23) (2003), 4140–4142.
225. Principa Partners; "Nanocomposites 1999: Polymer technology for the next century", Techn. Report, Principa Partners Consulting (1999).